
PUDLE: Implicit Acceleration of Dictionary Learning by Backpropagation

Bahareh Tolooshams

School of Engineering and Applied Sciences
Harvard University
btolooshams@seas.harvard.edu

Demba Ba

School of Engineering and Applied Sciences
Harvard University
demba@seas.harvard.edu

Abstract

The dictionary learning problem, representing data as a combination of few atoms, has long stood as a popular method for learning representations in statistics and signal processing. The most popular dictionary learning algorithm alternates between sparse coding and dictionary update steps, and a rich literature has studied its theoretical convergence. The growing popularity of neurally plausible unfolded sparse coding networks has led to the empirical finding that backpropagation through such networks performs dictionary learning. This paper offers the first theoretical proof for these empirical results through PUDLE, a Provable Unfolded Dictionary LEarning method. We highlight the impact of loss, unfolding, and backpropagation on convergence. We discover an implicit acceleration: as a function of unfolding, the backpropagated gradient converges faster and is more accurate than the gradient from alternating minimization. We complement our findings through synthetic and image denoising experiments. The findings support the use of accelerated deep learning optimizers and unfolded networks for dictionary learning.

1 Introduction

This paper considers the *dictionary learning* problem, namely representing data $\mathbf{x} \in \mathcal{X} \subset \mathbb{R}^m$ as linear combinations of a few atoms from a dictionary $\mathbf{D} \in \mathcal{D} \subset \mathbb{R}^{m \times p}$. Given \mathbf{x} and \mathbf{D} , the problem of recovering the sparse (few non-zero elements) coefficients $\mathbf{z} \in \mathbb{R}^p$ is referred to as *sparse coding* which can be solved through the lasso [1] (also known as basis pursuit [2]):

$$\ell_{\mathbf{x}}(\mathbf{D}) := \min_{\mathbf{z} \in \mathbb{R}^p} \mathcal{L}_{\mathbf{x}}(\mathbf{z}, \mathbf{D}) + h(\mathbf{z}) \quad (1)$$

where $\mathcal{L}_{\mathbf{x}}(\mathbf{z}, \mathbf{D}) = \frac{1}{2} \|\mathbf{x} - \mathbf{D}\mathbf{z}\|_2^2$, and $h(\mathbf{z}) = \lambda \|\mathbf{z}\|_1$. From the perspective of statistical learning, the dictionary of interest comprises the atoms that minimize the *expected risk*, i.e.,

$$\mathbf{D}^* \in \arg \min_{\mathbf{D} \in \mathcal{D}} \mathbb{E}_{\mathbf{x} \in \mathcal{X}} [\ell_{\mathbf{x}}(\mathbf{D})]. \quad (2)$$

The signal processing literature typically assumes a dictionary $\tilde{\mathbf{D}}$ that *generates* the data, i.e.,

$$\mathbf{x} = \tilde{\mathbf{D}}\tilde{\mathbf{z}} \quad (3)$$

where $\tilde{\mathbf{z}}$ is sparse, and aims to recover $\tilde{\mathbf{D}}$. Olshausen and Field [3] introduced (3) in computational neuroscience as a model for how early layers of the visual cortex process natural images. Sparse coding has been widely studied and utilized in the statistics [4] and signal processing communities [5]. Practical examples are denoising [6], super-resolution [7], and classification [8], where it enables the extraction of sparse high-dimensional features representing data. Furthermore, sparse coding has been utilized to construct neural architectures through approaches such as sparse energy-based models [9, 10] or recurrent sparsifying encoders [11]. The latter has initiated a growing literature on constructing deep networks based on an approach referred to as algorithm unfolding [12, 13]. Deep

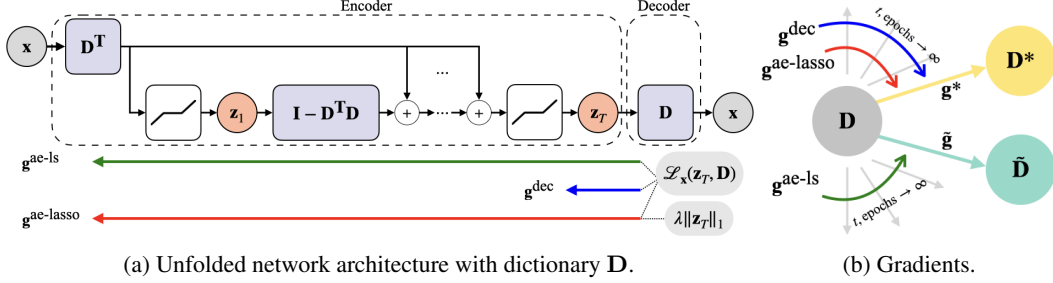


Figure 1: Provable unfolded dictionary learning (PUDLE).

unfolded neural networks have gained popularity in recent years due to their computational efficiency and their performance in various domains such as image denoising [14, 15, 16], super-resolution [17], medical imaging [18], deblurring [19, 20], and speech processing [12].

Prior to the advent of unfolded networks, gradient-based dictionary learning relied on analytic gradients computed from the lasso given the sparse code. With unfolded networks, automatic differentiation [21], referred to as backpropagation [22] in the reverse-mode, gained attention for parameter estimation [23, 15, 16]. The automatic gradient is obtained by backpropagation through the algorithm used to estimate the code. Automatic differentiation in reverse and forward-mode [24] is used in other areas, e.g., hyperparameter selection [25], and in a more relevant context, in the seminal work of LISTA [11]. Other works demonstrated empirically the convergence of dictionary learning by backpropagation through unfolded networks [15, 23]. Despite the empirical evidence, there is no known theoretical analysis of backpropagation in unfolded networks for *dictionary learning*.

This paper proposes a Provable Unfolded Dictionary LEarning (PUDLE) (Figure 1a). Given finite computational power, sparse coding can be converted into an encoder obtained by unfolding T iterations of ISTA [26, 27]. The decoder is a linear map reconstructing the data [23]. We adopt the perspective of (3) and aim to recover \tilde{D} by training the network using backpropagation with a learning rate of η . Three different choices affect the gradient: the loss, the number of unfolded iterations, and whether one backpropagates through decoder or through *both* the encoder and decoder.

This paper highlights the impact of such choices on the convergence of the training algorithm. Backpropagation through the decoder results in the analytic gradient g_t^{dec} using the code estimate z_t . The gradients $g_t^{\text{ae-lasso}}$ and $g_t^{\text{ae-ls}}$ are computed by backpropagation through the autoencoder using the lasso and least-squares objectives, respectively (Algorithm 2). We compare Algorithm 2 with the classical gradient-based alternating-minimization algorithm for dictionary learning [28], which cycles between sparse coding and dictionary update steps using the analytic gradient \hat{g} Algorithm 1.

Contributions We study gradient estimations (Figure 1b) for dictionary learning in PUDLE.

- **Implicit acceleration:** We prove that $g_t^{\text{ae-lasso}}$ converges to \hat{g} faster than g_t^{dec} . We refer to this as *implicit acceleration*. Hence, given a reasonable finite number of unfoldings, $g_t^{\text{ae-lasso}}$ is a better estimator than g_t^{dec} , resulting in convergence to a closer neighbourhood of D^* (Theorem 3.3).
- **Dictionary learning:** Given fixed λ , g_t^{dec} and $g_t^{\text{ae-lasso}}$ point towards D^* . $g_t^{\text{ae-ls}}$ is a better estimator of the direction to recover \tilde{D} than the other two gradients. Hence, $g_t^{\text{ae-ls}}$ converges to a closer neighbourhood of \tilde{D} than others (Theorem 3.4).
- **Unbiased estimation:** We show that the biased estimation of \tilde{D} vanishes as $\lambda_t = \lambda\beta^t$ (with $0 < \beta < 1$) decays within the unfolded layers (Figure 6).
- **Image denoising:** In a supervised image denoising task, we show that the advantage of $g_t^{\text{ae-ls}}$ goes beyond dictionary learning. Additionally, our network outperforms the sparse coding scheme in NOODL, a state-of-the-art online dictionary learning algorithm [29] (Table 1).
- **Neural plausibility:** Prior works have mainly focused on the neural plausibility of sparse coding and designed a dictionary gradient update independent of the coding step [30, 29]. PUDLE highlights a link between the neural plausibility of sparse coding and the dictionary update. Specifically, we show that backpropagating through the sparse coding step yields an implicit gradient update rule and eliminates the need for explicit ones.

Related works *Implicit acceleration* is termed *super efficiency* in [31], which compares analytic and automatic gradient estimators of min-min or max-min optimizations with smooth and differentiable functions. Unlike our work, where we evaluate the gradients for global model recovery, Ablin et al. study the asymptotic error of the gradients locally in each step of an alternating minimization [31].

There is a vast literature on the theoretical convergence of dictionary learning. Spielman et al. proposed a factorization method to recover the dictionary in the undercomplete setting (i.e., $p \leq m$) [32]. Barak et al. proposed to solve dictionary learning via sum-of-squares semidefinite program [33]. K-SVD [34] and MOD [35] are popular greedy approaches. Alternating-minimization-based methods have been used extensively both in theory and in practice [36, 37, 38].

Recent work has incorporated gradient-based updates into alternating minimization [28, 30, 29]. Chatterji and Bartlett provided a finite sample analysis and convergence guarantees when updating the dictionary using the analytic gradient [28]. Arora et al. proposed and studied neurally plausible dictionary learning approaches with analytic gradients [30]. A follow-up work focused on online dictionary learning [39] with an unbiased gradient for dictionary update [29]. Arora et al. discussed methods to reduce the bias of dictionary estimation [30], and Rambhatla et al. showed how to reduce bias in both code and dictionary estimations [29]. A common feature in the above-mentioned work is the use of analytic gradients, instead of automatic ones. Indeed, the previous works explicitly design tailored gradient updates independent of the sparse coding step and do not utilize backpropagation with deep learning optimizers. A theoretical analysis of backpropagation for dictionary learning exists only for shallow ReLU autencoders [40, 41].

The theoretical analysis of unfolded neural networks has mainly analyzed the convergence speed of variants of LISTA [11], where the focus is on *sparse coding* (i.e., the encoder) not *dictionary learning* [42, 43, 44, 45, 46, 47, 48]. Moreau and Bruna showed that upon successful factorization of the Gram matrix of the dictionary within layers, the network achieves accelerated convergence [44]. Giryes et al. examined the tradeoffs between reconstruction accuracy and convergence speed of LISTA [45]. Moreover, Chen et al. studied the learning dynamics of the weights and biases of unfolded-ISTA and proved that it achieves linear convergence [46]. Follow-up works investigated the dynamics of step-size in a recursive sparse coding encoder [47, 48]. Ablin et al. minimized the lasso through backpropagation but still assumed the knowledge of the dictionary at the decoder [48].

Notation Bold-lower-case and upper-case letters refer to vectors \mathbf{d} and matrices \mathbf{D} . We use \mathbf{d}_j to denote the j^{th} element of the vector \mathbf{d} , and \mathbf{D}_j is the j^{th} column of the matrix \mathbf{D} . $\lambda > 0$ is the regularization (sparsity-enforcing) parameter. $\sigma_{\max}(\mathbf{D})$ is the maximum singular value of \mathbf{D} . When taking the derivatives or norms w.r.t the matrix \mathbf{D} , we assume that \mathbf{D} is vectorized. $\nabla_1 \mathcal{L}(\mathbf{z}, \mathbf{D})$ and $\nabla_2 \mathcal{L}(\mathbf{z}, \mathbf{D})$ are the first derivatives of the loss w.r.t \mathbf{z} and \mathbf{D} , respectively. $\nabla_{11}^2 \mathcal{L}(\mathbf{z}, \mathbf{D})$ is the second derivative of the loss w.r.t \mathbf{z} . $\nabla_{21}^2 \mathcal{L}(\mathbf{z}, \mathbf{D})$ is the derivative of $\nabla_1 \mathcal{L}(\mathbf{z}, \mathbf{D})$ w.r.t \mathbf{D} . The support of \mathbf{z} is $\text{supp}(\mathbf{z}) \triangleq \{j: \mathbf{z}_j \neq 0\}$. We denote $\{1, \dots, p\}$ by $[1, p]$.

2 Preliminaries

Given n independent samples, dictionary learning aims to minimize the *empirical risk*, i.e.,

$$\min_{\mathbf{D} \in \mathcal{D}} \mathcal{R}_n(\mathbf{D}) \quad \text{with} \quad \mathcal{R}_n(\mathbf{D}) \triangleq \frac{1}{n} \sum_{i=1}^n \ell_{\mathbf{x}^i}(\mathbf{D}) \quad (4)$$

where $\lim_{n \rightarrow \infty} \mathcal{R}_n(\mathbf{D}) = \mathbb{E}_{\mathbf{x} \in \mathcal{X}} [\ell_{\mathbf{x}}(\mathbf{D})]$ a.s. To prevent scaling ambiguity between the code \mathbf{z} and dictionary \mathbf{D} , it is common to constrain the norm of the dictionary columns. Hence, we define the set of feasible solutions for the dictionary as $\mathcal{D} \triangleq \{\mathbf{D} \in \mathbb{R}^{m \times p} \text{ s.t. } \forall j \in [1, p], \|\mathbf{D}_j\|_2^2 \leq 1\}$. We can project estimates of \mathbf{D} onto the feasible set by performing $\mathbf{D}_j \leftarrow \frac{1}{\max(\|\mathbf{D}_j\|_2, 1)} \mathbf{D}_j$, either at every update or at the end of training. We assume certain properties on the domain of the data and dictionary (Assumption 2.1), as well as a bound on the energy of the data (Assumption 2.2).

Assumption 2.1 (Domain signals). \mathcal{X} and \mathcal{D} are both compact convex sets.

Assumption 2.2 (Bounded signals). $\exists M > 0$ s.t. $\|\mathbf{x}\|_2 < M \forall \mathbf{x} \in \mathcal{X}$.

The recurrent encoder and decoder, which perform the computations shown in Algorithm 2, use the loss \mathcal{L} and proximal operator $\mathcal{P}_{\alpha h}(v) \triangleq \text{sign}(v) \max(|v| - \alpha\lambda, 0)$ for the ℓ_1 norm $h: \mathbb{R}^p \rightarrow \mathbb{R}$. The encoder implements ISTA [26, 27] with step-size α , assumed to be less than $1/\sigma_{\max}^2(\mathbf{D})$. With infinite encoder unfolding, the encoder's output is the solution to the lasso (1), following the optimality

condition (Lemma A.3) where we denote $f_{\mathbf{x}}(\mathbf{z}, \mathbf{D}) \triangleq \mathcal{L}_{\mathbf{x}}(\mathbf{z}, \mathbf{D}) + h(\mathbf{z})$. One immediate observation is that $\lambda \geq \|\mathbf{D}^T \mathbf{x}\|_{\infty} \Leftrightarrow \{\mathbf{0}\} \in \arg \min f_{\mathbf{x}}(\mathbf{z}, \mathbf{D})$. We assume $\lambda < \|\mathbf{D}^T \mathbf{x}\|_{\infty}$ and the solution to (1) is unique. Sufficient conditions for uniqueness in the overcomplete case (i.e., $p > m$) are extensively studied in the literature [49, 50, 51]. Tibshirani discussed that the solution is unique with probability one if entries of \mathbf{D} are drawn from a continuous probability distribution [51] (Assumption 2.3). We argue that as long as the data $\mathbf{x} \in \mathcal{X}$ are sampled from a continuous distribution, this assumption holds for the entire learning process. The assumption has been previously considered in analyses of unfolded sparse coding networks [48] and can be extended to ℓ_1 regularized optimization problems [51, 52].

Assumption 2.3 (Lasso uniqueness). *The entries of the dictionary \mathbf{D} are continuously distributed. Hence, the minimizer of (1) is unique, i.e., $\{\hat{\mathbf{z}}\} \in \arg \min f_{\mathbf{x}}(\mathbf{z}, \mathbf{D})$ with probability one.*

Lemma 2.1 states the fixed-point property of the encoder recursion [53]. Given the definitions for Lipschitz and Lipschitz differentiable functions, (Definitions A.1 and A.2), the loss \mathcal{L} and function h satisfy following Lipschitz properties, which will play an important role in our analysis.

Lemma 2.1 (Fixed-point property of lasso). *Given Assumption 2.3, we have $\mathbf{0} \in \nabla_1 \mathcal{L}(\hat{\mathbf{z}}, \mathbf{D}) + \partial h(\hat{\mathbf{z}})$. The minimizer is a fixed-point of the mapping, i.e., $\hat{\mathbf{z}} = \mathcal{P}_{\alpha h}(\hat{\mathbf{z}} - \alpha \nabla_1 \mathcal{L}(\hat{\mathbf{z}}, \mathbf{D})) = \Phi(\hat{\mathbf{z}})$ [53].*

Lemma 2.2 (Lipschitz differentiable least squares). *Given $\mathcal{L}_{\mathbf{x}}(\mathbf{z}, \mathbf{D}) = \frac{1}{2} \|\mathbf{x} - \mathbf{D}\mathbf{z}\|_2^2$, \mathcal{D} , and Assumption 2.2, the loss is Lipschitz differentiable. Let L_1 and L_2 denote the Lipschitz constants of the first derivatives $\nabla_1 \mathcal{L}_{\mathbf{x}}(\mathbf{z}, \mathbf{D})$ and $\nabla_2 \mathcal{L}_{\mathbf{x}}(\mathbf{z}, \mathbf{D})$, L_{11} and L_{21} the Lipschitz constants of the second derivatives $\nabla_{11}^2 \mathcal{L}_{\mathbf{x}}(\mathbf{z}, \mathbf{D})$ and $\nabla_{21}^2 \mathcal{L}_{\mathbf{x}}(\mathbf{z}, \mathbf{D})$, all w.r.t \mathbf{z} . Let $\nabla_1 \mathcal{L}_{\mathbf{x}}(\mathbf{z}, \mathbf{D})$ be L_D -Lipschitz w.r.t \mathbf{D} .*

Lemma 2.3 (Lipschitz proximal). *Given $h(\mathbf{z}) = \lambda \|\mathbf{z}\|_1$, its proximal operator has bounded sub-derivative, i.e., $\|\partial \mathcal{P}_h(\mathbf{z})\|_2 \leq c_{prox}$.*

3 Main Results

The gradients defined in PUDLE (Algorithm 2) can be compared against the local direction at each update of classical alternating-minimization (Algorithm 1). Assuming there are infinite samples, i.e.,

$$\text{Best local direction : } \hat{\mathbf{g}} \triangleq \lim_{n \rightarrow \infty} \frac{1}{n} \sum_{i=1}^n \nabla_2 \mathcal{L}_{\mathbf{x}^i}(\hat{\mathbf{z}}^i, \mathbf{D}) = \mathbb{E}_{\mathbf{x} \in \mathcal{X}} [\nabla_2 \mathcal{L}_{\mathbf{x}}(\hat{\mathbf{z}}, \mathbf{D})] \quad (5)$$

where $\hat{\mathbf{z}} = \arg \min_{\mathbf{z} \in \mathbb{R}^p} \mathcal{L}_{\mathbf{x}}(\mathbf{z}, \mathbf{D}) + h(\mathbf{z})$. Additionally, to assess the estimators for model recovery, hence dictionary learning, we compare them against gradients that point towards \mathbf{D}^* and $\tilde{\mathbf{D}}$, namely

$$\begin{aligned} \text{Desired gradient for } \mathbf{D}^* : \quad \mathbf{g}^* &\triangleq \lim_{n \rightarrow \infty} \frac{1}{n} \sum_{i=1}^n \nabla_2 \mathcal{L}_{\mathbf{x}^i}(\mathbf{z}^{i*}, \mathbf{D}) = \mathbb{E}_{\mathbf{x} \in \mathcal{X}} [\nabla_2 \mathcal{L}_{\mathbf{x}}(\mathbf{z}^*, \mathbf{D})] \\ \text{Desired gradient for } \tilde{\mathbf{D}} : \quad \tilde{\mathbf{g}} &\triangleq \lim_{n \rightarrow \infty} \frac{1}{n} \sum_{i=1}^n \nabla_2 \mathcal{L}_{\mathbf{x}^i}(\tilde{\mathbf{z}}^i, \mathbf{D}) = \mathbb{E}_{\mathbf{x} \in \mathcal{X}} [\nabla_2 \mathcal{L}_{\mathbf{x}}(\tilde{\mathbf{z}}, \mathbf{D})] \end{aligned} \quad (6)$$

where $\mathbf{z}^* = \arg \min_{\mathbf{z} \in \mathbb{R}^p} \mathcal{L}_{\mathbf{x}}(\mathbf{z}, \mathbf{D}^*) + h(\mathbf{z})$. To see why the above are desired directions, we highlight that $(\mathbf{z}^*, \mathbf{D}^*)$ is a critical point of the *expected risk*. Hence, given the current \mathbf{D} , to reach the critical point by gradient descent, we move towards the direction minimizing $\mathbb{E}_{\mathbf{x} \in \mathcal{X}} [\mathcal{L}_{\mathbf{x}}(\mathbf{z}^*, \mathbf{D})]$. Similarly, $(\tilde{\mathbf{z}}, \tilde{\mathbf{D}})$ is a critical point of the loss \mathcal{L} which also reaches zero for data following the model (3). Hence, to reach $\tilde{\mathbf{D}} \in \arg \min_{\mathbf{D} \in \mathcal{D}} \mathbb{E}_{\mathbf{x} \in \mathcal{X}} [\mathcal{L}_{\mathbf{x}}(\tilde{\mathbf{z}}, \mathbf{D})]$, we move towards the direction minimizing the loss in expectation. Given these directions, we analyze the error of the gradients $\mathbf{g}_t^{\text{dec}}$, $\mathbf{g}_t^{\text{ae-lasso}}$, and $\mathbf{g}_t^{\text{ae-ls}}$ assuming infinite samples. In this regard, we first study the forward pass.

3.1 Forward pass

We show two convergence results in the forward pass, one for \mathbf{z} and another for the Jacobian, i.e.,

Definition 3.1 (Code Jacobian). *Given \mathbf{D} , the Jacobian of \mathbf{z}_t is defined as $\mathbf{J}_t \triangleq \frac{\partial \mathbf{z}_t}{\partial \mathbf{D}}$.*

The forward pass analysis gives upper bounds on the error between \mathbf{z}_t and $\hat{\mathbf{z}}$ and the error between \mathbf{J}_t and $\hat{\mathbf{J}}$ as a function of unfolded iterations t . We will require these errors in Section 3.2, where we analyze the gradient estimation errors. Similar to [28], the error associated with $\mathbf{g}_t^{\text{dec}}$ depends on the code convergence. Unlike $\mathbf{g}_t^{\text{dec}}$, the convergence of backpropagation with gradient estimates $\mathbf{g}_t^{\text{ae-lasso}}$ and $\mathbf{g}_t^{\text{ae-ls}}$ relies on the convergence properties of the code *and* the Jacobian [31]. Forward-pass theories are based on studies by Gilbert on the convergence of variables and their derivatives in an iterative process governed by a smooth operator [54]. Moreover, Hale et al. studied the convergence analysis of fixed point iterations for ℓ_1 regularized optimization problems [55]. In Proposition 3.1, we re-state a result from [55] on support selection.

Algorithm 1: Classical alternating-minimization-based dictionary learning using lasso (1).

Initialize: Samples $\{\mathbf{x}^i\}_{i=1}^n \in \mathcal{X}$, initial dictionary $\mathbf{D}^{(0)}$

Repeat: $l = 0, 1, \dots$, number of epochs

Sparse coding step: $\mathbf{z}^{i(l)} = \arg \min_{\mathbf{z}} \mathcal{L}_{\mathbf{x}^i}(\mathbf{z}, \mathbf{D}^{(l)}) + h(\mathbf{z})$, (for $i \in [1, n]$)

Dictionary update: $\mathbf{D}^{(l+1)} = \mathbf{D}^{(l)} - \eta \hat{\mathbf{g}}^{(l)}$ where $\hat{\mathbf{g}}^{(l)} \triangleq \frac{1}{n} \sum_{i=1}^n \nabla_2 \mathcal{L}_{\mathbf{x}^i}(\mathbf{z}^{i(l)}, \mathbf{D}^{(l)})$

Algorithm 2: PUDLE: Provable unfolded dictionary learning framework.

Initialize: Samples $\{\mathbf{x}^i\}_{i=1}^n \in \mathcal{X}$, initial dictionary $\mathbf{D}^{(0)}$, and $\mathbf{z}_0 = \mathbf{0}$.

Repeat: $l = 0, 1, \dots$, number of epochs

Forward pass: (for $i \in [1, n]$)

$$\begin{aligned} \text{Encoder: } \mathbf{z}_{t+1}^{i(l)} &= \Phi(\mathbf{z}_t^{i(l)}, \mathbf{D}^{(l)}) = \mathcal{P}_{\alpha h}(\mathbf{z}_t^{i(l)} - \alpha \nabla_1 \mathcal{L}_{\mathbf{x}^i}(\mathbf{z}_t^{i(l)}, \mathbf{D}^{(l)})) \text{ (repeat for } T) \\ \text{Decoder: } \hat{\mathbf{x}}^{i(l)} &= \mathbf{D}^{(l)} \mathbf{z}_T^{i(l)} \end{aligned} \quad (7)$$

Backward pass: $\mathbf{D}^{(l+1)} = \mathbf{D}^{(l)} - \eta \mathbf{g}_T^{(l)}$ where $\mathbf{g}_T^{(l)}$ is either of

$$\begin{aligned} \mathbf{g}_t^{(l) \text{ dec}} &\triangleq \frac{1}{n} \sum_{i=1}^n \nabla_2 \mathcal{L}_{\mathbf{x}^i}(\mathbf{z}_t^{i(l)}, \mathbf{D}^{(l)}) \\ \mathbf{g}_t^{(l) \text{ ae-lasso}} &\triangleq \frac{1}{n} \sum_{i=1}^n \nabla_2 \mathcal{L}_{\mathbf{x}^i}(\mathbf{z}_t^{i(l)}, \mathbf{D}^{(l)}) + \frac{\partial \mathbf{z}_t^{i(l)}}{\partial \mathbf{D}^{(l)}} \left(\nabla_1 \mathcal{L}_{\mathbf{x}^i}(\mathbf{z}_t^{i(l)}, \mathbf{D}^{(l)}) + \partial h(\mathbf{z}_t^{i(l)}) \right) \\ \mathbf{g}_t^{(l) \text{ ae-ls}} &\triangleq \frac{1}{n} \sum_{i=1}^n \nabla_2 \mathcal{L}_{\mathbf{x}^i}(\mathbf{z}_t^{i(l)}, \mathbf{D}^{(l)}) + \frac{\partial \mathbf{z}_t^{i(l)}}{\partial \mathbf{D}^{(l)}} \nabla_1 \mathcal{L}_{\mathbf{x}^i}(\mathbf{z}_t^{i(l)}, \mathbf{D}^{(l)}) \end{aligned} \quad (8)$$

Proposition 3.1 (Finite-iteration support selection). *Given Assumption 2.3, let $\hat{\mathbf{z}} = \arg \min_{\mathbf{z}} f_{\mathbf{x}}(\mathbf{z}, \mathbf{D})$ with $S \triangleq \text{supp}(\hat{\mathbf{z}})$. There exists a $B > 0$ such that $\text{supp}(\mathbf{z}_B) = S, \forall t > B$.*

This means that the unfolded encoder identifies the support in finite iterations. Support recovery in finite iterations has been studied in the literature for LISTA [46], Step-LISTA [48], and shallow autoencoders [30, 40, 41, 16]. We now state Theorem 3.1 on the rate of convergence of the encoder.

Theorem 3.1 (Forward pass code convergence). *Given the iterative encoder $\mathbf{z}_{t+1} = \Phi(\mathbf{z}_t, \mathbf{D})$, Assumption 2.3, and Lemmas 2.1, A.1 and A.2,*

$$\exists \rho < 1, B > 0 \quad \text{s.t.} \quad \|\mathbf{z}_t - \hat{\mathbf{z}}\|_2 \leq O(\rho^t) \quad \forall t > B \quad (9)$$

where $\hat{\mathbf{z}}$ is the unique minimizer of lasso (1).

Proof sketch (full details in Appendix A.1). Given the finite-iteration support selection property (Proposition 3.1), we show the strong convexity of \mathcal{L} w.r.t \mathbf{z} restricted to the support for $t > B$ (Lemma A.1). This property allows us to bound the sub-derivative of the recursion $\mathbf{z}_{t+1} = \Phi(\mathbf{z}_t, \mathbf{D})$ for $t > B$ (Lemma A.2). We then use the fixed-point property of the encoder (Lemma 2.1) to find an upper bound on $\|\mathbf{z}_t - \hat{\mathbf{z}}\|_2$ for $t > B$ which goes to 0 as $t \rightarrow \infty$. ■

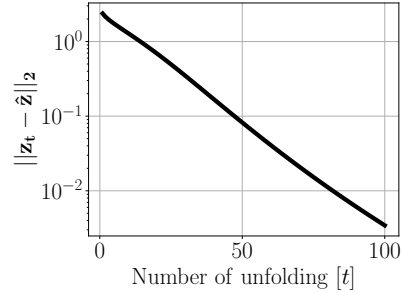


Figure 2: Results for code convergence (Theorem 3.1) demonstrating that as the PUDLE network unfolds, \mathbf{z}_t converges to $\hat{\mathbf{z}}$, the solution of lasso.

Remarks Theorem 3.1 shows that in PUDLE, \mathbf{z}_t converges to $\hat{\mathbf{z}}$ at a linear rate eventually after a certain number of unfoldings (Figure 2). The local linear convergence of ISTA and FISTA [56] in the neighbourhood of a fixed-point is studied in [57]. The speed of convergence depends on when support selection happens (Proposition 3.1) [58, 59]. Overall, the lasso converges at the global rate of $O(1/t)$ and $O(1/t^2)$ for ISTA and FISTA, respectively [56]. Chen et al. has proved that it is possible to attain linear convergence for all iterations given a LISTA encoder [46]. PUDLE is constrained for unsupervised dictionary learning; hence it differs from LISTA as we assume no knowledge of $\hat{\mathbf{z}}$.

Following properties similar to those used in Theorem 3.1, and assuming \mathbf{J}_t is bounded (Assumption 3.1), we show in Theorem 3.2 that, as the PUDLE unfolds, the code Jacobian \mathbf{J}_t converges to $\hat{\mathbf{J}}$,

the Jacobian of the solution of lasso. The convergence of the Jacobian of proximal gradient descent is also studied in [60] for hyperparameter selection through implicit differentiation [61]. In their case, the Jacobian is taken w.r.t to the hyperparameter λ as opposed to \mathbf{D} .

Assumption 3.1 (Bounded Jacobian). *The Jacobian is bounded, i.e., $\exists M_J > 0$, s.t. $\|\mathbf{J}_t\|_2 \leq M_J \forall t$.*

Theorem 3.2 (Forward pass Jacobian convergence). *Given the recursion $\mathbf{z}_{t+1} = \Phi(\mathbf{z}_t, \mathbf{D})$, and $\hat{\mathbf{z}}$ the unique minimizer of lasso with Jacobian $\hat{\mathbf{J}}$,*

$$\exists \rho < 1, B > 0 \quad \text{s.t.} \quad \|\mathbf{J}_t - \hat{\mathbf{J}}\|_2 \leq O(t\rho^{t-1}) \quad \forall t > B. \quad (10)$$

Proof sketch (full details in Appendix A.2). Differentiating the recursion, we get the relation $\mathbf{J}_{t+1} = \nabla_1 \Phi(\mathbf{z}_t, \mathbf{D})\mathbf{J}_t + \nabla_2 \Phi(\mathbf{z}_t, \mathbf{D})$. Using Lemma 2.1, we have $\hat{\mathbf{J}} = \nabla_1 \Phi(\hat{\mathbf{z}}, \mathbf{D})\hat{\mathbf{J}} + \nabla_2 \Phi(\hat{\mathbf{z}}, \mathbf{D})$. Then, we find an upper bound on $\|\mathbf{J}_t - \hat{\mathbf{J}}\|_2$, given the Lipschitz properties and the bounded Jacobian. ■

3.2 Backward pass

We show two results for local (relating to $\hat{\mathbf{g}}$) and global (relating to \mathbf{g}^* and $\tilde{\mathbf{g}}$) gradient convergence. The goal is not to provide a finite sample analysis but to emphasize the *relative* differences between the gradients in Algorithm 2. The impact of gradient error for parameter estimation has been studied by Devolder et al. indicating that the convergence to the parameter's neighbourhood is dictated by the gradient error [62, 63]. The intuition is that the size of the gradient error dictates the size of the neighbourhood of the dictionary within which one can guarantee convergence. We argue that the method with lower gradient error recovers the dictionary better. We drop the superscript (l) to simplify the notation.

Local gradient estimations We highlight the effect of finite computational capacity in the sparse coding step of PUDLE on the gradient for parameter estimation [31]. Theorem 3.3 shows the convergence rate of gradients to $\hat{\mathbf{g}}$, determining the similarity of PUDLE and Algorithm 1.

Theorem 3.3 (Local convergence of gradients). *Given the convergence results from the forward pass (Theorems 3.1 and 3.2), $\exists \rho < 1, B > 0$ such that $\forall t > B$, the errors of gradients defined in Algorithm 2 w.r.t $\hat{\mathbf{g}}$ (5) satisfy*

$$\begin{aligned} \|\mathbf{g}_t^{\text{dec}} - \hat{\mathbf{g}}\|_2 &\leq O(\rho^t) \\ \|\mathbf{g}_t^{\text{ae-lasso}} - \hat{\mathbf{g}}\|_2 &\leq O(t\rho^{2t-1}) \\ \|\mathbf{g}_t^{\text{ae-ls}} - \hat{\mathbf{g}}\|_2 &\leq O(t\rho^{2t-1} + \hat{C}_h) \end{aligned} \quad (11)$$

where \hat{C}_h is an upper bound on $M_J \|\partial h(\hat{\mathbf{z}})\|_2$.

Remarks First, upper bounds on the errors related to $\mathbf{g}_t^{\text{dec}}$ and $\mathbf{g}_t^{\text{ae-lasso}}$ go to zero as t increases. Hence, both gradients converge to $\hat{\mathbf{g}}$. This means that asymptotically as t increases, training PUDLE with $\mathbf{g}_t^{\text{dec}}$ and $\mathbf{g}_t^{\text{ae-lasso}}$ is equivalent to classical alternating-minimization (Algorithm 1). Second, as t increases, $\mathbf{g}_t^{\text{ae-lasso}}$ has faster convergence than $\mathbf{g}_t^{\text{dec}}$. Lastly, $\mathbf{g}_t^{\text{ae-ls}}$ is a biased estimator of $\hat{\mathbf{g}}$ Figure 3.

Proof sketch (full details in Appendix A.3). The error for $\mathbf{g}_t^{\text{dec}}$ can be bounded using the constant L_2 . Given infinite samples, we replace the sample mean with expectation in their limit. We use the property $\mathbf{0} \in \nabla_1 \mathcal{L}_{\mathbf{x}}(\hat{\mathbf{z}}, \mathbf{D}) + \partial h(\hat{\mathbf{z}})$. For $\mathbf{g}_t^{\text{ae-lasso}}$ and $\mathbf{g}_t^{\text{ae-ls}}$, we re-write the gradient errors as

$$\begin{aligned} \mathbf{g}_t^{\text{ae-lasso}} - \hat{\mathbf{g}} &= \mathbb{E}_{\mathbf{x} \in \mathcal{X}} [Q(\hat{\mathbf{z}}, \mathbf{J}_t)(\mathbf{z}_t - \hat{\mathbf{z}})] + \mathbb{E}_{\mathbf{x} \in \mathcal{X}} [Q_t^{21}(\hat{\mathbf{z}})] + \mathbb{E}_{\mathbf{x} \in \mathcal{X}} [\mathbf{J}_t Q_t^{\text{lasso-11}}(\hat{\mathbf{z}})] \\ \mathbf{g}_t^{\text{ae-ls}} - \hat{\mathbf{g}} &= \mathbb{E}_{\mathbf{x} \in \mathcal{X}} [Q(\hat{\mathbf{z}}, \mathbf{J}_t)(\mathbf{z}_t - \hat{\mathbf{z}})] + \mathbb{E}_{\mathbf{x} \in \mathcal{X}} [Q_t^{21}(\hat{\mathbf{z}})] + \mathbb{E}_{\mathbf{x} \in \mathcal{X}} [\mathbf{J}_t Q_t^{\text{ls-11}}(\hat{\mathbf{z}})] \end{aligned} \quad (12)$$

where

$$\begin{aligned} Q_t^{21}(\mathbf{z}) &\triangleq \nabla_2 \mathcal{L}_{\mathbf{x}}(\mathbf{z}_t, \mathbf{D}) - \nabla_2 \mathcal{L}_{\mathbf{x}}(\mathbf{z}, \mathbf{D}) - \nabla_{21}^2 \mathcal{L}_{\mathbf{x}}(\mathbf{z}, \mathbf{D})(\mathbf{z}_t - \mathbf{z}) \\ Q_t^{\text{lasso-11}}(\mathbf{z}) &\triangleq \nabla_1 \mathcal{L}_{\mathbf{x}}(\mathbf{z}_t, \mathbf{D}) + \partial h(\mathbf{z}_t) - \nabla_{11}^2 \mathcal{L}_{\mathbf{x}}(\mathbf{z}, \mathbf{D})(\mathbf{z}_t - \mathbf{z}) \\ Q_t^{\text{ls-11}}(\mathbf{z}) &\triangleq \nabla_1 \mathcal{L}_{\mathbf{x}}(\mathbf{z}_t, \mathbf{D}) - \nabla_{11}^2 \mathcal{L}_{\mathbf{x}}(\mathbf{z}, \mathbf{D})(\mathbf{z}_t - \mathbf{z}) \\ Q(\mathbf{z}, \mathbf{J}) &\triangleq \mathbf{J} \nabla_{11}^2 \mathcal{L}_{\mathbf{x}}(\mathbf{z}, \mathbf{D}) + \nabla_{21}^2 \mathcal{L}_{\mathbf{x}}(\mathbf{z}, \mathbf{D}). \end{aligned} \quad (13)$$

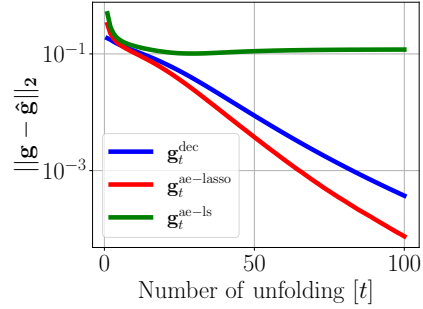


Figure 3: Results for the convergence rate of PUDLE gradients (Theorem 3.3). $\mathbf{g}_t^{\text{dec}}$ converges to $\hat{\mathbf{g}}$ at a linear rate after certain t , $\mathbf{g}_t^{\text{ae-lasso}}$ converges faster, and $\mathbf{g}_t^{\text{ae-ls}}$ is its biased estimator.

Hence, it suffices to bound the terms on the *r.h.s* using [Assumption 3.1](#) and [Lemma 3.1](#). \blacksquare

Lemma 3.1 (Local bounds). *From local gradient errors in [Theorem 3.3](#), the following are satisfied*

$$\begin{aligned} \|Q_t^{21}(\hat{\mathbf{z}})\|_2 &\leq (L_{21}/2)\|\mathbf{z}_t - \hat{\mathbf{z}}\|_2^2, & \|Q_t^{lasso-11}(\hat{\mathbf{z}})\|_2 &\leq (L_{11}/2)\|\mathbf{z}_t - \hat{\mathbf{z}}\|_2^2 \\ \|Q(\hat{\mathbf{z}}, \mathbf{J}_t)\|_2 &\leq L_1\|\mathbf{J}_t - \hat{\mathbf{J}}\|_2, & \|Q_t^{ls-11}(\hat{\mathbf{z}})\|_2 &\leq (L_{11}/2)\|\mathbf{z}_t - \hat{\mathbf{z}}\|_2^2 + \|\partial h(\hat{\mathbf{z}})\|_2. \end{aligned} \quad (14)$$

Global gradient estimations [Theorem 3.4](#) shows the global gradient errors w.r.t \mathbf{g}^* and $\tilde{\mathbf{g}}$ from (6). This result determines whether the PUDLE gradients facilitate the recovery of \mathbf{D}^* or $\tilde{\mathbf{D}}$ [62, 63].

Theorem 3.4 (Global convergence of gradients). *Given the convergence results from the forward pass, ([Theorems 3.1](#) and [3.2](#)), $\exists \rho < 1, B > 0$ such that $\forall t > B$, the errors of gradients defined in [Algorithm 2](#) w.r.t global directions \mathbf{g}^* and $\tilde{\mathbf{g}}$ (defined in (6)) satisfy*

$$\begin{aligned} \|\mathbf{g}_t^{dec} - \mathbf{g}^*\|_2 &\leq O(\rho^t + C_z^*) \\ \|\mathbf{g}_t^{ae-lasso} - \mathbf{g}^*\|_2 &\leq O(t\rho^{2t-1} + C_z^*t\rho^{t-1} + \rho^t C_J^* + (C_z^* + 1)C_J^* + C_D^*) \\ \|\mathbf{g}_t^{ae-ls} - \mathbf{g}^*\|_2 &\leq O(t\rho^{2t-1} + C_z^*t\rho^{t-1} + \rho^t C_J^* + (C_z^* + 1)C_J^* + C_D^* + C_h^*) \end{aligned} \quad (15)$$

$$\begin{aligned} \|\mathbf{g}_t^{dec} - \tilde{\mathbf{g}}\|_2 &\leq O(\rho^t + \tilde{C}_z) \\ \|\mathbf{g}_t^{ae-lasso} - \tilde{\mathbf{g}}\|_2 &\leq O(t\rho^{2t-1} + \tilde{C}_z t\rho^{t-1} + \rho^t \tilde{C}_J + (\tilde{C}_z + 1)\tilde{C}_J + \tilde{C}_D + C_h^t) \\ \|\mathbf{g}_t^{ae-ls} - \tilde{\mathbf{g}}\|_2 &\leq O(t\rho^{2t-1} + \tilde{C}_z t\rho^{t-1} + \rho^t \tilde{C}_J + (\tilde{C}_z + 1)\tilde{C}_J + \tilde{C}_D) \end{aligned} \quad (16)$$

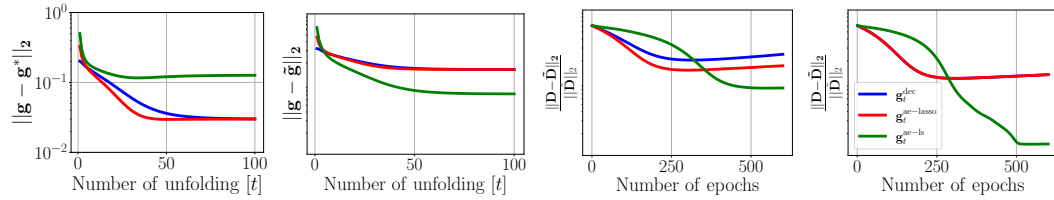
where $C_z^* \triangleq O(\|\hat{\mathbf{z}} - \mathbf{z}^*\|_2)$, $C_J^* \triangleq O(\|\hat{\mathbf{J}} - \mathbf{J}^*\|_2)$, $C_D^* \triangleq O(\|\mathbf{D} - \mathbf{D}^*\|_2)$, and C_h^* is an upper bound on $M_J \|\partial h(\mathbf{z}^*)\|_2$. Similarly, we have $\tilde{C}_z \triangleq O(\|\hat{\mathbf{z}} - \tilde{\mathbf{z}}\|_2)$, $\tilde{C}_J^* \triangleq O(\|\hat{\mathbf{J}} - \tilde{\mathbf{J}}\|_2)$, $\tilde{C}_D^* \triangleq O(\|\mathbf{D} - \tilde{\mathbf{D}}\|_2)$, and C_h^t is an upper bound on $M_J \|\partial h(\mathbf{z}_t)\|_2$.

Remarks Several factors affect the upper bounds in [Theorem 3.4](#): the number of unfolded iterations, the current estimate of the dictionary, code, Jacobian and, more importantly, the sub-derivative of ℓ_1 norm. As we analyzed the effect of unfolding in [Theorem 3.3](#), let us study the bounds as $t \rightarrow \infty$. In this case, \mathbf{g}_∞^{dec} and $\mathbf{g}_\infty^{ae-lasso}$ are equivalent, so we compare only $\mathbf{g}_\infty^{ae-lasso}$ with $\mathbf{g}_\infty^{ae-ls}$. We have

$$\begin{aligned} \|\mathbf{g}_\infty^{ae-lasso} - \mathbf{g}^*\|_2 &\leq O(C^*), & \|\mathbf{g}_\infty^{ae-lasso} - \tilde{\mathbf{g}}\|_2 &\leq O(\tilde{C} + C_h^\infty) \\ \|\mathbf{g}_\infty^{ae-ls} - \mathbf{g}^*\|_2 &\leq O(C^* + C_h^*), & \|\mathbf{g}_\infty^{ae-ls} - \tilde{\mathbf{g}}\|_2 &\leq O(\tilde{C}) \end{aligned} \quad (17)$$

where $C^* \triangleq (C_z^* + 1)C_J^* + C_D^*$, and $\tilde{C} \triangleq (\tilde{C}_z + 1)\tilde{C}_J + \tilde{C}_D$. For errors w.r.t \mathbf{g}^* , the upper bound on $\mathbf{g}_\infty^{ae-ls}$ has an extra term (i.e., C_h^*) compared to $\mathbf{g}_\infty^{ae-lasso}$. This highlights that $\mathbf{g}_\infty^{ae-lasso}$ is a better estimator of \mathbf{g}^* ([Figure 4a](#)). Similarly, we argue that $\mathbf{g}_\infty^{ae-ls}$ is a better estimator of $\tilde{\mathbf{g}}$ ([Figure 4b](#)).

Implications of such gradient estimation are seen in dictionary learning where $\mathbf{g}_\infty^{ae-ls}$ recovers $\tilde{\mathbf{D}}$ better ([Figures 4c](#) and [4d](#)). In [Figure 4c](#), the encoder unfolds for $T = 25$, hence the phenomenon of *implicit acceleration* is seen in *faster and better* dictionary learning performance of $\mathbf{g}_\infty^{ae-lasso}$ than \mathbf{g}_∞^{dec} . In [Figure 4d](#) where $T = 100$, similar performance of \mathbf{g}_∞^{dec} and $\mathbf{g}_\infty^{ae-lasso}$ illustrates their asymptotic equivalence as $t \rightarrow \infty$. Additionally, we observed that the learned dictionary by \mathbf{g}_∞^{dec} and $\mathbf{g}_\infty^{ae-lasso}$ is closer to \mathbf{D}^* than $\tilde{\mathbf{D}}$. This is reversed for $\mathbf{g}_\infty^{ae-ls}$, i.e., the learned dictionary is closer to $\tilde{\mathbf{D}}$.



(a) Convergence for \mathbf{g}^* . (b) Convergence for $\tilde{\mathbf{g}}$. (c) Learning ($T = 25$). (d) Learning ($T = 100$).

Figure 4: Results for PUDLE's global convergence ([Theorem 3.4](#)) and dictionary learning.

Proof sketch (full details in Appendix A.5). Given infinite samples, we replace the sample mean with expectation in their limit. The proof is similar to Theorem 3.3. The key difference is that we first upper bound the errors w.r.t $\|\mathbf{z}_t - \mathbf{z}^*\|_2$ and $\|\mathbf{z}_t - \tilde{\mathbf{z}}\|_2$. More importantly, in this case, $\mathbf{0} \in \nabla_1 \mathcal{L}_{\mathbf{x}}(\mathbf{z}^*, \mathbf{D}^*) + \partial h(\mathbf{z}^*)$ and $\mathbf{0} = \nabla_1 \mathcal{L}_{\mathbf{x}}(\tilde{\mathbf{z}}, \tilde{\mathbf{D}})$. We bound the error for $\mathbf{g}_t^{\text{dec}}$ using the constant L_2 . We re-write the errors of gradients $\mathbf{g}_t^{\text{ae-lasso}}$ and $\mathbf{g}_t^{\text{ae-ls}}$ as following

$$\begin{aligned} \mathbf{g}_t^{\text{ae-lasso}} - \mathbf{g}^* &= \mathbb{E}_{\mathbf{x} \in \mathcal{X}} [Q(\mathbf{z}^*, \mathbf{J}_t)(\mathbf{z}_t - \mathbf{z}^*)] + \mathbb{E}_{\mathbf{x} \in \mathcal{X}} [Q_t^{21}(\mathbf{z}^*)] + \mathbb{E}_{\mathbf{x} \in \mathcal{X}} [\mathbf{J}_t Q_t^{\text{lasso-11}}(\mathbf{z}^*)] \\ \mathbf{g}_t^{\text{ae-ls}} - \mathbf{g}^* &= \mathbb{E}_{\mathbf{x} \in \mathcal{X}} [Q(\mathbf{z}^*, \mathbf{J}_t)(\mathbf{z}_t - \mathbf{z}^*)] + \mathbb{E}_{\mathbf{x} \in \mathcal{X}} [Q_t^{21}(\mathbf{z}^*)] + \mathbb{E}_{\mathbf{x} \in \mathcal{X}} [\mathbf{J}_t Q_t^{\text{ls-11}}(\mathbf{z}^*)] \end{aligned} \quad (18)$$

$$\begin{aligned} \mathbf{g}_t^{\text{ae-lasso}} - \tilde{\mathbf{g}} &= \mathbb{E}_{\mathbf{x} \in \mathcal{X}} [Q(\tilde{\mathbf{z}}, \mathbf{J}_t)(\mathbf{z}_t - \tilde{\mathbf{z}})] + \mathbb{E}_{\mathbf{x} \in \mathcal{X}} [Q_t^{21}(\tilde{\mathbf{z}})] + \mathbb{E}_{\mathbf{x} \in \mathcal{X}} [\mathbf{J}_t Q_t^{\text{lasso-11}}(\tilde{\mathbf{z}})] \\ \mathbf{g}_t^{\text{ae-ls}} - \tilde{\mathbf{g}} &= \mathbb{E}_{\mathbf{x} \in \mathcal{X}} [Q(\tilde{\mathbf{z}}, \mathbf{J}_t)(\mathbf{z}_t - \tilde{\mathbf{z}})] + \mathbb{E}_{\mathbf{x} \in \mathcal{X}} [Q_t^{21}(\tilde{\mathbf{z}})] + \mathbb{E}_{\mathbf{x} \in \mathcal{X}} [\mathbf{J}_t Q_t^{\text{ls-11}}(\tilde{\mathbf{z}})] \end{aligned} \quad (19)$$

where $Q_t^{21}(\mathbf{z})$, $Q_t^{\text{lasso-11}}(\mathbf{z})$, $Q_t^{\text{ls-11}}(\mathbf{z})$, and $Q(\mathbf{z}, \mathbf{J})$ are defined as in Theorem 3.3. Given Assumption 3.1 and Lemma 3.2, we find an upper bound on *r.h.s.* \blacksquare

Lemma 3.2 (Global bounds). *From global gradient errors in Theorem 3.4, the following are satisfied*

$$\begin{aligned} \|Q_t^{21}(\mathbf{z}^*)\|_2 &\leq (L_{21}/2)\|\mathbf{z}_t - \mathbf{z}^*\|_2^2 \\ \|Q_t^{\text{lasso-11}}(\mathbf{z}^*)\|_2 &\leq (L_{11}/2)\|\mathbf{z}_t - \mathbf{z}^*\|_2^2 + L_D\|\mathbf{D} - \mathbf{D}^*\|_2 \\ \|Q_t^{\text{ls-11}}(\mathbf{z}^*)\|_2 &\leq (L_{11}/2)\|\mathbf{z}_t - \mathbf{z}^*\|_2^2 + L_D\|\mathbf{D} - \mathbf{D}^*\|_2 + \|\partial h(\mathbf{z}^*)\|_2 \\ \|Q(\mathbf{z}^*, \mathbf{J}_t)\|_2 &\leq L_1\|\mathbf{J}_t - \mathbf{J}^*\|_2 \end{aligned} \quad (20)$$

$$\begin{aligned} \|Q_t^{21}(\tilde{\mathbf{z}})\|_2 &\leq (L_{21}/2)\|\mathbf{z}_t - \tilde{\mathbf{z}}\|_2^2 \\ \|Q_t^{\text{lasso-11}}(\tilde{\mathbf{z}})\|_2 &\leq (L_{11}/2)\|\mathbf{z}_t - \tilde{\mathbf{z}}\|_2^2 + L_D\|\mathbf{D} - \tilde{\mathbf{D}}\|_2 + \|\partial h(\mathbf{z}_t)\|_2 \\ \|Q_t^{\text{ls-11}}(\tilde{\mathbf{z}})\|_2 &\leq (L_{11}/2)\|\mathbf{z}_t - \tilde{\mathbf{z}}\|_2^2 + L_D\|\mathbf{D} - \tilde{\mathbf{D}}\|_2 \\ \|Q(\tilde{\mathbf{z}}, \mathbf{J}_t)\|_2 &\leq L_1\|\mathbf{J}_t - \tilde{\mathbf{J}}\|_2. \end{aligned} \quad (21)$$

Towards unbiased estimation As long as λ is fixed within the PUDLE architecture, all defined gradients remain biased estimators of $\tilde{\mathbf{g}}$, due to the biased estimation of the code $\tilde{\mathbf{z}}$ through ℓ_1 norm. This bias exists as long as dictionary learning is performed strictly using *lasso* through Algorithm 1. We empirically show in Section 4 that by decaying λ at each unfolded layer, this bias vanishes, and the training converges to $\tilde{\mathbf{D}}$. We conjecture that in this case the sequence of $\mathbf{D}^*(\lambda_t)$ converges to $\tilde{\mathbf{D}}$. We leave the theoretical analysis of this setting for future work.

Beyond dictionary learning Our results are founded on three main properties: Lipschitz differentiability of the loss relating to the parameter of interest, proximal gradient descent, and strong convexity in finite-iteration. The findings can be applied to other min-min optimization problems, e.g., ridge regression and logistic regression, following such properties. For example, our analysis generalizes to the unfolded network in [16] for learning dictionaries using data from the natural exponential family. In this case, the least-squares loss is replaced with negative log-likelihood, and the dictionary models the expectation of the data [16].

Limitations Finite-iteration support selection (Proposition 3.1) [55] and strong convexity may seem stringent going beyond dictionary learning. Ablin et al. briefly discuss generalization of local gradient convergence by relaxing strong convexity to the p -Łojasiewicz property [31, 64]. Although our analysis considered only the noiseless setting, we conjecture that the relative comparison of the gradients in the presence of noise still holds, where the upper bounds will involve an additional term related to the noise. This paper focused on infinite sample convergence as the goal was to highlight the relative differences between the gradients. With more assumptions on the code statistics, finite-sample upper bounds can be derived similar to [28, 30].

4 Experiments

Dictionary learning We focus on the performance of our best-performing gradient estimators $\mathbf{g}_t^{\text{ae-ls}}$, and compare it with NOODL [29], a state-of-the-art online algorithm, and SPORCO [65], an alternating-minimization algorithm that uses lasso. NOODL, which

uses iterative hard-thresholding (HT) for sparse coding and a gradient update employing the code’s sign, has linear convergence upon proper initialization [29]. We train:

- $\mathbf{g}_t^{\text{ae-ls}}$: λ is fixed across iterations.
- $\mathbf{g}_t^{\text{ae-ls, decay}}$: λ decays (i.e., $\lambda_t = \lambda\beta^t$, with $0 < \beta < 1$) where β decreases as training progresses.
- $\mathbf{g}_t^{\text{ae-ls, HT}}$: $\mathcal{P}_{\alpha h}(v)$ is replaced with $\text{HT}_b(v) \triangleq v\mathbf{1}_{|v|\geq b}$.

The intuition behind decreasing λ across iterations is to have an unbiased estimation of the code amplitudes. With HT, the sparse coding step reduces to that from NOODL. In this case, we highlight the difference between the gradient update of our method (backpropagation) with NOODL.

Figure 5 shows the convergence of $\mathbf{D} \in \mathbb{R}^{1000 \times 1500}$ to $\tilde{\mathbf{D}}$ for when the code is 20-sparse (for other sparsity levels and details see Appendix B). A biased estimation of the code amplitudes results in convergence only to a neighbourhood of the dictionary [29]. This is observed in the convergence of SPORCO (final error is shown) and $\mathbf{g}_t^{\text{ae-ls}}$. The convergence of $\mathbf{g}_t^{\text{ae-ls}}$ to a closer neighbourhood than SPORCO supports Theorem 3.4. Moreover, with decaying λ , the code estimation bias vanishes, hence $\mathbf{g}_t^{\text{ae-ls, decay}}$ and $\mathbf{g}_t^{\text{ae-ls, HT}}$ converges to $\tilde{\mathbf{D}}$ similar to NOODL. Here, we focus on convergence, as η across methods is not comparable.

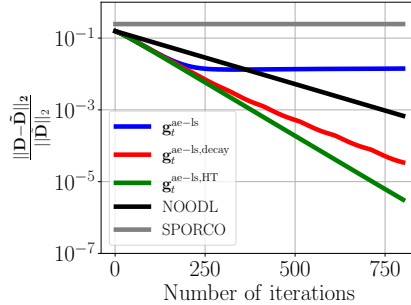


Figure 5: Dictionary convergence of $\mathbf{g}_t^{\text{ae-ls}}$, NOODL [29] and SPORCO [65].

Supervised image denoising We focus on $\mathbf{g}_t^{\text{ae-ls}}$ and $\mathbf{g}_t^{\text{dec}}$ to highlight the impact of backpropagation, and also consider $\mathbf{g}_t^{\text{ae-ls, HT}}$ where the proximal operator is replaced with HT. This is to compare with sparse coding scheme of NOODL. We do not compare against NOODL’s dictionary update, as this computation for two-dimensional convolutions is not straightforward. Prior works have shown that variants of PUDLE either rival or outperform state-of-the-art architectures for image denoising [14, 16]. Thus, we focus on a comparative analysis of the gradients. We trained on 432 and tested on 68 images from BSD [66]. We used a convolutional dictionary and corrupted images with zero-mean Gaussian noise of standard deviation of 25 (see Appendix B for details). Table 1 shows the denoising performance of soft-thresholding using λ , and HT with b in peak signal-to-noise-ratio (PSNR). The result shows that the advantage of $\mathbf{g}_t^{\text{ae-ls}}$ over $\mathbf{g}_t^{\text{dec}}$ is not limited to dictionary learning and is seen in denoising. Additionally, the superior performance of $\mathbf{g}_t^{\text{ae-ls}}$ compared to $\mathbf{g}_t^{\text{ae-ls, HT}}$ highlights the advantage of PUDLE (i.e., ℓ_1 -based unfolding) against HT used in NOODL.

Table 1: Denoising of BSD68 [66].

Method	PSNR [dB]			
λ	0.08	0.12	0.16	0.2
$\mathbf{g}_t^{\text{dec}}$	24.31	24.73	25.24	24.89
$\mathbf{g}_t^{\text{ae-ls}}$	24.80	25.48	25.67	25.51
b	0.02	0.05	0.08	0.1
$\mathbf{g}_t^{\text{ae-ls, HT}}$	22.87	25.40	24.68	23.77

5 Conclusions

This paper studied dictionary learning and analyzed the dynamics of unfolded sparse coding networks through a provable unfolded dictionary learning (PUDLE) framework. We provided the first theoretical results on network convergence when trained by backpropagation. The results highlight the interplay between neural plausibility of sparse coding and dictionary learning, specifically the effect of learning the dictionary by backpropagation through the sparse coding step. We proved how backpropagation exhibits an implicit acceleration of gradient convergence and dictionary learning as a function of unfolded sparse coding iterations, compared to classical alternating-minimization-based gradients. We showed how the loss function can ameliorate the gradient bias. We demonstrated that this bias could be further reduced and eliminated by decaying the regularization parameter within the unfolded layers. We showed that this result goes beyond dictionary learning where PUDLE outperforms the NOODL sparse coding scheme in an image denoising task [29].

References

- [1] R. Tibshirani, “Regression shrinkage and selection via the lasso,” *Journal of the Royal Statistical Society. Series B (Methodological)*, vol. 58, no. 1, pp. 267–288, 1996.
- [2] S. S. Chen, D. L. Donoho, and M. A. Saunders, “Atomic decomposition by basis pursuit,” *SIAM review*, vol. 43, no. 1, pp. 129–159, 2001.
- [3] B. A. Olshausen and D. J. Field, “Sparse coding with an overcomplete basis set: A strategy employed by v1?” *Vision research*, vol. 37, no. 23, pp. 3311–3325, 1997.
- [4] T. Hastie, R. Tibshirani, and M. Wainwright, *Statistical learning with sparsity: the lasso and generalizations*. CRC press, 2015.
- [5] M. Elad, *Sparse and redundant representations: from theory to applications in signal and image processing*. Springer Science & Business Media, 2010.
- [6] M. Elad and M. Aharon, “Image denoising via sparse and redundant representations over learned dictionaries,” *IEEE Transactions on Image Processing*, vol. 15, no. 12, pp. 3736–3745, 2006.
- [7] J. Yang, J. Wright, T. S. Huang, and Y. Ma, “Image super-resolution via sparse representation,” *IEEE Transactions on Image Processing*, vol. 19, no. 11, pp. 2861–2873, 2010.
- [8] J. Mairal, J. Ponce, G. Sapiro, A. Zisserman, and F. Bach, “Supervised dictionary learning,” in *Proc. Advances in Neural Information Processing Systems*, vol. 21, 2009, pp. 1–8.
- [9] M. a. Ranzato, C. Poultney, S. Chopra, and Y. Cun, “Efficient learning of sparse representations with an energy-based model,” in *Advances in Neural Information Processing Systems*, vol. 19. MIT Press, 2007.
- [10] M. a. Ranzato, Y.-I. Boureau, and Y. Cun, “Sparse feature learning for deep belief networks,” in *Proc. Advances in Neural Information Processing Systems*, J. Platt, D. Koller, Y. Singer, and S. Roweis, Eds., vol. 20, 2008.
- [11] K. Gregor and Y. LeCun, “Learning fast approximations of sparse coding,” in *Proc. international conference on international conference on machine learning*, 2010, pp. 399–406.
- [12] J. R. Hershey, J. L. Roux, and F. Weninger, “Deep unfolding: Model-based inspiration of novel deep architectures,” *arXiv:1409.2574*, pp. 1–27, 2014.
- [13] V. Monga, Y. Li, and Y. C. Eldar, “Algorithm unrolling: Interpretable, efficient deep learning for signal and image processing,” *arXiv:1912.10557*, pp. 1–27, 2019.
- [14] D. Simon and M. Elad, “Rethinking the csc model for natural images,” in *Proc. Advances in Neural Information Processing Systems*, vol. 32, 2019, pp. 1–11.
- [15] B. Tolooshams, S. Dey, and D. Ba, “Deep residual autoencoders for expectation maximization-inspired dictionary learning,” *IEEE Transactions on Neural Networks and Learning Systems*, pp. 1–15, 2020.
- [16] B. Tolooshams, A. H. Song, S. Temereanca, and D. Ba, “Convolutional dictionary learning based autoencoders for natural exponential-family distributions,” in *Proc. International Conference on Machine Learning*, 2020, pp. 1–11.
- [17] Z. Wang, D. Liu, J. Yang, W. Han, and T. Huang, “Deep networks for image super-resolution with sparse prior,” in *Proc. IEEE International Conference on Computer Vision*, 2015, pp. 370–378.
- [18] O. Solomon, R. Cohen, Y. Zhang, Y. Yang, Q. He, J. Luo, R. J. G. van Sloun, and Y. C. Eldar, “Deep unfolded robust pca with application to clutter suppression in ultrasound,” *IEEE Transactions on Medical Imaging*, vol. 39, no. 4, pp. 1051–1063, 2020.
- [19] C. J. Schuler, M. Hirsch, S. Harmeling, and B. Schölkopf, “Learning to deblur,” *IEEE Transactions on Pattern Analysis and Machine Intelligence*, vol. 38, no. 7, pp. 1439–1451, 2016.
- [20] Y. Li, M. Tofighi, J. Geng, V. Monga, and Y. C. Eldar, “Efficient and interpretable deep blind image deblurring via algorithm unrolling,” *IEEE Transactions on Computational Imaging*, vol. 6, pp. 666–681, 2020.
- [21] A. G. Baydin, B. A. Pearlmutter, A. A. Radul, and J. M. Siskind, “Automatic differentiation in machine learning: a survey,” *Journal of machine learning research*, vol. 18, 2018.
- [22] Y. A. LeCun, L. Bottou, G. B. Orr, and K.-R. Müller, “Efficient backprop,” in *Neural networks: Tricks of the trade*. Springer, 2012, pp. 9–48.
- [23] B. Tolooshams, S. Dey, and D. Ba, “Scalable convolutional dictionary learning with constrained recurrent sparse auto-encoders,” in *Proc. IEEE International Workshop on Machine Learning for Signal Processing*, 2018, pp. 1–6.
- [24] L. Franceschi, M. Donini, P. Frasconi, and M. Pontil, “Forward and reverse gradient-based hyperparameter optimization,” in *Proc. International Conference on Machine Learning*, 2017, pp. 1165–1173.

- [25] M. Feurer and F. Hutter, “Hyperparameter optimization,” in *Automated Machine Learning*. Springer, Cham, 2019, pp. 3–33.
- [26] I. Daubechies, M. Defrise, and C. De Mol, “An iterative thresholding algorithm for linear inverse problems with a sparsity constraint,” *Communications on Pure and Applied Mathematics*, vol. 57, no. 11, pp. 1413–1457, 2004.
- [27] T. Blumensath and M. E. Davies, “Iterative thresholding for sparse approximations,” *Journal of Fourier analysis and Applications*, vol. 14, no. 5-6, pp. 629–654, 2008.
- [28] N. S. Chatterji and P. L. Bartlett, “Alternating minimization for dictionary learning: Local convergence guarantees,” *arXiv:1711.03634*, pp. 1–26, 2017.
- [29] S. Rambhatla, X. Li, and J. Haupt, “Noodl: Provable online dictionary learning and sparse coding,” in *Proc. International Conference on Learning Representations*, 2018, pp. 1–11.
- [30] S. Arora, R. Ge, T. Ma, and A. Moitra, “Simple, efficient, and neural algorithms for sparse coding,” in *Proc. Conference on Learning Theory*, ser. Proc. Machine Learning Research, P. Grünwald, E. Hazan, and S. Kale, Eds., vol. 40. Paris, France: PMLR, 03–06 Jul 2015, pp. 113–149.
- [31] P. Ablin, G. Peyré, and T. Moreau, “Super-efficiency of automatic differentiation for functions defined as a minimum,” in *Proc. International Conference on Machine Learning*. PMLR, 2020, pp. 32–41.
- [32] D. A. Spielman, H. Wang, and J. Wright, “Exact recovery of sparsely-used dictionaries,” in *Proc. Annual Conference on Learning Theory*, ser. PMRL, vol. 23, 2012, pp. 37.1–37.18.
- [33] B. Barak, J. A. Kelner, and D. Steurer, “Dictionary learning and tensor decomposition via the sum-of-squares method,” in *Proc. Annual ACM Symposium on Theory of Computing*, ser. STOC ’15, 2015, p. 143–151.
- [34] M. Aharon, M. Elad, and A. Bruckstein, “K-svd: An algorithm for designing overcomplete dictionaries for sparse representation,” *IEEE Transactions on Signal Processing*, vol. 54, no. 11, pp. 4311–4322, 2006.
- [35] K. Engan, S. Aase, and J. Hakon Husoy, “Method of optimal directions for frame design,” in *Proc. IEEE International Conference on Acoustics, Speech, and Signal Processing*, vol. 5, 1999, pp. 2443–2446 vol.5.
- [36] P. Jain, P. Netrapalli, and S. Sanghavi, “Low-rank matrix completion using alternating minimization,” in *Proc. Annual ACM Symposium on Theory of Computing*, 2013, p. 665–674.
- [37] A. Agarwal, A. Anandkumar, P. Jain, P. Netrapalli, and R. Tandon, “Learning sparsely used overcomplete dictionaries,” in *Proc the 27th Conference on Learning Theory*, ser. Proc. Machine Learning Research, M. F. Balcan, V. Feldman, and C. Szepesvári, Eds., vol. 35. Barcelona, Spain: PMLR, 13–15 Jun 2014, pp. 123–137.
- [38] S. Arora, R. Ge, and A. Moitra, “New algorithms for learning incoherent and overcomplete dictionaries,” in *Proc. the 27th Conference on Learning Theory*, ser. Proc. Machine Learning Research, M. F. Balcan, V. Feldman, and C. Szepesvári, Eds., vol. 35. Barcelona, Spain: PMLR, 13–15 Jun 2014, pp. 779–806.
- [39] J. Mairal, F. Bach, J. Ponce, and G. Sapiro, “Online dictionary learning for sparse coding,” in *Proc. Annual International Conference on Machine Learning*, 2009, p. 689–696.
- [40] A. Rangamani, A. Mukherjee, A. Basu, A. Arora, T. Ganapathi, S. Chin, and T. D. Tran, “Sparse coding and autoencoders,” in *Proc. IEEE International Symposium on Information Theory (ISIT)*, 2018, pp. 36–40.
- [41] T. V. Nguyen, R. K. Wong, and C. Hegde, “On the dynamics of gradient descent for autoencoders,” in *Proc. International Conference on Artificial Intelligence and Statistics*. PMLR, 2019, pp. 2858–2867.
- [42] P. Sprechmann, A. Bronstein, and G. Sapiro, “Learning efficient structured sparse models,” in *Proc. International Conference on International Conference on Machine Learning*, 2012, p. 219–226.
- [43] B. Xin, Y. Wang, W. Gao, D. Wipf, and B. Wang, “Maximal sparsity with deep networks?” in *Advances in Neural Information Processing Systems*, D. Lee, M. Sugiyama, U. Luxburg, I. Guyon, and R. Garnett, Eds., vol. 29, 2016, pp. 1–9.
- [44] T. Moreau and J. Bruna, “Understanding trainable sparse coding via matrix factorization,” in *Proc. 5th International Conference on Learning Representations*, 2017, pp. 1–13.
- [45] R. Giryes, Y. C. Eldar, A. M. Bronstein, and G. Sapiro, “Tradeoffs between convergence speed and reconstruction accuracy in inverse problems,” *IEEE Transactions on Signal Processing*, vol. 66, no. 7, pp. 1676–1690, 2018.
- [46] X. Chen, J. Liu, Z. Wang, and W. Yin, “Theoretical linear convergence of unfolded ista and its practical weights and thresholds,” in *Proc. Advances in Neural Information Processing Systems*, vol. 31, 2018, pp. 1–11.
- [47] J. Liu and X. Chen, “Alista: Analytic weights are as good as learned weights in lista,” in *Proc. International Conference on Learning Representations*, 2019.

- [48] P. Ablin, T. Moreau, M. Massias, and A. Gramfort, “Learning step sizes for unfolded sparse coding,” in *Proc. Advances in Neural Information Processing Systems*, vol. 32, 2019, pp. 1–11.
- [49] M. J. Wainwright, “Sharp thresholds for high-dimensional and noisy sparsity recovery using ℓ_1 -constrained quadratic programming (lasso),” *IEEE transactions on information theory*, vol. 55, no. 5, pp. 2183–2202, 2009.
- [50] E. J. Candès and Y. Plan, “Near-ideal model selection by ℓ_1 minimization,” *The Annals of Statistics*, vol. 37, no. 5A, pp. 2145 – 2177, 2009.
- [51] R. J. Tibshirani, “The lasso problem and uniqueness,” *Electronic Journal of Statistics*, vol. 7, no. none, pp. 1456 –1490, 2013.
- [52] S. Rosset, J. Zhu, and T. Hastie, “Boosting as a regularized path to a maximum margin classifier,” *The Journal of Machine Learning Research*, vol. 5, pp. 941–973, 2004.
- [53] N. Parikh and S. Boyd, “Proximal algorithms,” *Foundations and Trends in optimization*, vol. 1, no. 3, pp. 127–239, 2014.
- [54] J. C. Gilbert, “Automatic differentiation and iterative processes,” *Optimization methods and software*, vol. 1, no. 1, pp. 13–21, 1992.
- [55] E. T. Hale, W. Yin, and Y. Zhang, “A fixed-point continuation method for ℓ_1 -regularized minimization with applications to compressed sensing,” *CAAM TR07-07, Rice University*, vol. 43, p. 44, 2007.
- [56] A. Beck and M. Teboulle, “A fast iterative shrinkage-thresholding algorithm for linear inverse problems,” *SIAM journal on imaging sciences*, vol. 2, no. 1, pp. 183–202, 2009.
- [57] S. Tao, D. Boley, and S. Zhang, “Local linear convergence of ista and fista on the lasso problem,” *SIAM Journal on Optimization*, vol. 26, no. 1, pp. 313–336, 2016.
- [58] K. Bredies and D. A. Lorenz, “Linear convergence of iterative soft-thresholding,” *Journal of Fourier Analysis and Applications*, vol. 14, no. 5-6, pp. 813–837, 2008.
- [59] L. Zhang, Y. Hu, C. Li, and J.-C. Yao, “A new linear convergence result for the iterative soft thresholding algorithm,” *Optimization*, vol. 66, no. 7, pp. 1177–1189, 2017.
- [60] Q. Bertrand, Q. Kloppenstein, M. Massias, M. Blondel, S. Vaiter, A. Gramfort, and J. Salmon, “Implicit differentiation for fast hyperparameter selection in non-smooth convex learning,” *arXiv:2105.01637*, 2021.
- [61] Y. Bengio, “Gradient-based optimization of hyperparameters,” *Neural computation*, vol. 12, no. 8, pp. 1889–1900, 2000.
- [62] O. Devolder, F. Glineur, Y. Nesterov *et al.*, “First-order methods with inexact oracle: the strongly convex case,” Université catholique de Louvain, Center for Operations Research and . . . , Tech. Rep., 2013.
- [63] O. Devolder, F. Glineur, and Y. Nesterov, “First-order methods of smooth convex optimization with inexact oracle,” *Mathematical Programming*, vol. 146, no. 1, pp. 37–75, 2014.
- [64] H. Attouch and J. Bolte, “On the convergence of the proximal algorithm for nonsmooth functions involving analytic features,” *Mathematical Programming*, vol. 116, no. 1, pp. 5–16, 2009.
- [65] B. Wohlberg, “Sporco: A python package for standard and convolutional sparse representations,” in *Proc. the 15th Python in Science Conference, Austin, TX, USA*, 2017, pp. 1–8.
- [66] D. Martin, C. Fowlkes, D. Tal, and J. Malik, “A database of human segmented natural images and its application to evaluating segmentation algorithms and measuring ecological statistics,” in *Proc. IEEE International Conference on Computer Vision*, vol. 2, 2001, pp. 416–423.
- [67] A. Paszke, S. Gross, S. Chintala, G. Chanan, E. Yang, Z. DeVito, Z. Lin, A. Desmaison, L. Antiga, and A. Lerer, “Automatic differentiation in pytorch,” 2017.
- [68] D. P. Kingma and J. Ba, “Adam: A method for stochastic optimization,” *arXiv:1412.6980*, 2014.

A Appendix

Definition A.1 (Lipschitz function). A function $f: \mathbb{R}^m \rightarrow \mathbb{R}^p$ is L -Lipschitz w.r.t a norm $\|\cdot\|$ if $\exists L > 0$ s.t. $\|f(a) - f(b)\| \leq L\|a - b\| \forall a, b \in \mathbb{R}^m$.

Definition A.2 (Lipschitz differentiable function). A twice differentiable function $f: \mathbb{R}^m \rightarrow \mathbb{R}^p$ is L -Lipschitz differentiable w.r.t a norm $\|\cdot\|$ iff $\exists L > 0$ s.t. $\|\nabla^2 f(a)\| \leq L \forall a \in \mathbb{R}^m$.

Definition A.3 (Strong convexity). A twice differentiable function $f: \mathbb{R}^m \rightarrow \mathbb{R}^p$ is strongly convex if $\exists \mu > 0$ s.t. $\nabla^2 f(a) \succeq \mu \mathbf{I}$.

Lemma A.1 (Strong convexity of reconstruction loss). Given the support selection ([Proposition 3.1](#)), $\mathbf{D}_S^T \mathbf{D}_S$ is full-rank. Thus, $\forall t > B$, $\mathcal{L}_{\mathbf{x}}(\mathbf{z}_t, \mathbf{D}) = \mathcal{L}_{\mathbf{x}}(\mathbf{z}_{t,S}, \mathbf{D}_S)$ is strongly convex ([Definition A.3](#)) in \mathbf{z} .

Lemma A.2 (Lipschitz mapping). Given the recursion $\mathbf{z}_{t+1} = \Phi(\mathbf{z}_t) = \mathcal{P}_{\alpha h}(\mathbf{z}_t - \alpha \nabla_1 \mathcal{L}_{\mathbf{x}}(\mathbf{z}_t, \mathbf{D}))$, from [Lemma A.1](#), there exist $B > 0$ such that loss $\mathcal{L}_{\mathbf{x}}(\mathbf{z}_t, \mathbf{D})$ is μ -strongly convex $\forall t > B$. Hence, using [Lemma 2.3](#),

$$\|\nabla_1 \Phi(\mathbf{z}_t, \mathbf{D})\|_2 = \|(\mathbf{I} - \alpha \nabla_{11}^2 \mathcal{L}(\mathbf{z}_t, \mathbf{D})) \partial \mathcal{P}_{\alpha h}(\mathbf{z}_t)\|_2 \leq \rho \quad (22)$$

where $\rho \triangleq c_{\text{prox}}(1 - \alpha\mu) < 1$.

Lemma A.3 (Lasso optimality). Lasso Karush-Kuhn-Tucker (KKT) optimality conditions are

$$\hat{\mathbf{z}} \in \arg \min_{\mathbf{z} \in \mathbb{R}^p} f_{\mathbf{x}}(\mathbf{z}, \mathbf{D}) \Leftrightarrow \mathbf{D}^T(\mathbf{x} - \mathbf{D}\hat{\mathbf{z}}) \in \lambda \partial \|\hat{\mathbf{z}}\|_1, \text{ and } |\hat{z}_j| = \begin{cases} \{\text{sign}(\hat{z}_j)\} & \text{if } \hat{z}_j \neq 0 \\ [-1, 1] & \text{if } \hat{z}_j = 0 \end{cases}, \forall j \in [1, p]. \quad (23)$$

A.1 Proof of [Theorem 3.1](#)

Theorem 3.1 (Forward pass code convergence). Given the iterative encoder $\mathbf{z}_{t+1} = \Phi(\mathbf{z}_t, \mathbf{D})$, [Assumption 2.3](#), and [Lemmas 2.1, A.1 and A.2](#),

$$\exists \rho < 1, B > 0 \quad \text{s.t.} \quad \|\mathbf{z}_t - \hat{\mathbf{z}}\|_2 \leq O(\rho^t) \quad \forall t > B \quad (9)$$

where $\hat{\mathbf{z}}$ is the unique minimizer of lasso (1).

Proof. Given the support selection at iteration B , from [Lemma A.1](#), we have $\nabla_{11}^2 \mathcal{L}(\mathbf{z}_t, \mathbf{D}) \succeq \mu \mathbf{I}$ restricted to the support for $t > B$. Then, from [Lemma A.2](#), we get

$$\|\nabla_1 \Phi(\mathbf{z}_t, \mathbf{D})\|_2 = \|(\mathbf{I} - \alpha \nabla_{11}^2 \mathcal{L}(\mathbf{z}_t, \mathbf{D})) \partial \mathcal{P}_{\alpha h}(\mathbf{z}_t)\|_2 \leq \rho$$

where $\rho \triangleq c_{\text{prox}}(1 - \alpha\mu) < 1$. Hence, using fixed-point property ([Lemma 2.1](#))

$$\exists B > 0, \text{ s.t. } \|\mathbf{z}_{t+1} - \hat{\mathbf{z}}\|_2 = \|\Phi(\mathbf{z}_t) - \Phi(\hat{\mathbf{z}})\|_2 \leq \rho \|\mathbf{z}_t - \hat{\mathbf{z}}\|_2 \quad \forall t > B$$

where $\hat{\mathbf{z}} = \arg \min f_{\mathbf{x}}(\mathbf{z}, \mathbf{D})$. Unrolling the recursion,

$$\|\mathbf{z}_t - \hat{\mathbf{z}}\|_2 \leq \rho^{t-B} \|\mathbf{z}_B - \hat{\mathbf{z}}\|_2. \quad \blacksquare$$

A.2 Proof of [Theorem 3.2](#)

Theorem 3.2 (Forward pass Jacobian convergence). Given the recursion $\mathbf{z}_{t+1} = \Phi(\mathbf{z}_t, \mathbf{D})$, and $\hat{\mathbf{z}}$ the unique minimizer of lasso with Jacobian $\hat{\mathbf{J}}$,

$$\exists \rho < 1, B > 0 \quad \text{s.t.} \quad \|\mathbf{J}_t - \hat{\mathbf{J}}\|_2 \leq O(t\rho^{t-1}) \quad \forall t > B. \quad (10)$$

Proof. Differentiating the recursion,

$$\mathbf{J}_{t+1} = \nabla_1 \Phi(\mathbf{z}_t, \mathbf{D}) \mathbf{J}_t + \nabla_2 \Phi(\mathbf{z}_t, \mathbf{D}).$$

Similarly,

$$\hat{\mathbf{J}} = \nabla_1 \Phi(\hat{\mathbf{z}}, \mathbf{D}) \hat{\mathbf{J}} + \nabla_2 \Phi(\hat{\mathbf{z}}, \mathbf{D})$$

where $\hat{\mathbf{z}}$ is a minimizer of lasso and fixed-point of the mapping (see [Lemma 2.1](#)). Subtract the terms $\mathbf{J}_{t+1} - \hat{\mathbf{J}} = \nabla_1 \Phi(\mathbf{z}_t, \mathbf{D})(\mathbf{J}_t - \hat{\mathbf{J}}) + (\nabla_1 \Phi(\mathbf{z}_t, \mathbf{D}) - \nabla_1 \Phi(\hat{\mathbf{z}}, \mathbf{D}))\hat{\mathbf{J}} + (\nabla_2 \Phi(\mathbf{z}_t, \mathbf{D}) - \nabla_2 \Phi(\hat{\mathbf{z}}, \mathbf{D}))$. Given the Lipschitz properties of \mathcal{L} and h , we can further get the upper bounds on $\|\nabla_1 \Phi(\mathbf{a}, \mathbf{D}) - \nabla_1 \Phi(\mathbf{b}, \mathbf{D})\|_2 \leq L_{\Phi_1}$ and $\|\nabla_2 \Phi(\mathbf{a}, \mathbf{D}) - \nabla_2 \Phi(\mathbf{b}, \mathbf{D})\|_2 \leq L_{\Phi_2}$. Hence, with upper bound on the norm of Jacobian ([Assumption 3.1](#)), there exists $B > 0$ such that $\forall t > B$

$$\begin{aligned} \|\mathbf{J}_{t+1} - \hat{\mathbf{J}}\|_2 &\leq \|\nabla_1 \Phi(\mathbf{z}_t, \mathbf{D})\|_2 \|\mathbf{J}_t - \hat{\mathbf{J}}\|_2 + \|\nabla_1 \Phi(\mathbf{z}_t, \mathbf{D}) - \nabla_1 \Phi(\hat{\mathbf{z}}, \mathbf{D})\|_2 \|\hat{\mathbf{J}}\|_2 \\ &\quad + \|\nabla_2 \Phi(\mathbf{z}_t, \mathbf{D}) - \nabla_2 \Phi(\hat{\mathbf{z}}, \mathbf{D})\|_2 \\ &\leq \rho \|\mathbf{J}_t - \hat{\mathbf{J}}\|_2 + c \|\mathbf{z}_t - \hat{\mathbf{z}}\|_2 \end{aligned}$$

where $c \triangleq M_J L_{\Phi_1} + L_{\Phi_2}$. Hence,

$$\|\mathbf{J}_{t+1} - \hat{\mathbf{J}}\|_2 \leq \rho \|\mathbf{J}_t - \hat{\mathbf{J}}\|_2 + O(\rho^t).$$

Unrolling the recursion,

$$\|\mathbf{J}_{t+1} - \hat{\mathbf{J}}\|_2 \leq O((t+1)\rho^t).$$

■

A.3 Proof of [Theorem 3.3](#)

Theorem 3.3 (Local convergence of gradients). *Given the convergence results from the forward pass ([Theorems 3.1 and 3.2](#)), $\exists \rho < 1, B > 0$ such that $\forall t > B$, the errors of gradients defined in [Algorithm 2](#) w.r.t $\hat{\mathbf{g}}$ ([5](#)) satisfy*

$$\begin{aligned} \|\mathbf{g}_t^{\text{dec}} - \hat{\mathbf{g}}\|_2 &\leq O(\rho^t) \\ \|\mathbf{g}_t^{\text{ae-lasso}} - \hat{\mathbf{g}}\|_2 &\leq O(t\rho^{2t-1}) \\ \|\mathbf{g}_t^{\text{ae-ls}} - \hat{\mathbf{g}}\|_2 &\leq O(t\rho^{2t-1} + \hat{C}_h) \end{aligned} \tag{11}$$

where \hat{C}_h is an upper bound on $M_J \|\partial h(\hat{\mathbf{z}})\|_2$.

Proof. For $\mathbf{g}_t^{\text{dec}}$, with the infinite fresh samples, we have $\lim_{n \rightarrow \infty} \frac{1}{n} \sum_{i=1}^n \nabla_2 \mathcal{L}_{\mathbf{x}^i}(\mathbf{z}_t^i, \mathbf{D}) = \mathbb{E}_{\mathbf{x} \in \mathcal{X}} [\nabla_2 \mathcal{L}_{\mathbf{x}}(\mathbf{z}_t, \mathbf{D})]$ a.s. Based on [Lemma 2.2](#), we get

$$\begin{aligned} \|\mathbf{g}_t^{\text{dec}} - \hat{\mathbf{g}}\|_2 &= \|\mathbb{E}_{\mathbf{x} \in \mathcal{X}} [\nabla_2 \mathcal{L}_{\mathbf{x}}(\mathbf{z}_t, \mathbf{D})] - \mathbb{E}_{\mathbf{x} \in \mathcal{X}} [\nabla_2 \mathcal{L}_{\mathbf{x}}(\hat{\mathbf{z}}, \mathbf{D})]\|_2 \\ &\leq \mathbb{E}_{\mathbf{x} \in \mathcal{X}} [\|\nabla_2 \mathcal{L}_{\mathbf{x}}(\mathbf{z}_t, \mathbf{D}) - \nabla_2 \mathcal{L}_{\mathbf{x}}(\hat{\mathbf{z}}, \mathbf{D})\|_2] \leq \mathbb{E}_{\mathbf{x} \in \mathcal{X}} [L_2 \|\mathbf{z}_t - \hat{\mathbf{z}}\|_2] \leq O(\rho^t). \end{aligned} \tag{24}$$

Similarly, for $\mathbf{g}_t^{\text{ae-lasso}}$ and $\mathbf{g}_t^{\text{ae-ls}}$, we replace the sample mean for gradient computations with expectation in their limit. We re-write the gradient estimation error as following

$$\begin{aligned} \mathbf{g}_t^{\text{ae-lasso}} - \hat{\mathbf{g}} &= \mathbb{E}_{\mathbf{x} \in \mathcal{X}} [Q(\hat{\mathbf{z}}, \mathbf{J}_t)(\mathbf{z}_t - \hat{\mathbf{z}})] + \mathbb{E}_{\mathbf{x} \in \mathcal{X}} [Q_t^{21}(\hat{\mathbf{z}})] + \mathbb{E}_{\mathbf{x} \in \mathcal{X}} [\mathbf{J}_t Q_t^{\text{lasso-11}}(\hat{\mathbf{z}})] \\ \mathbf{g}_t^{\text{ae-ls}} - \hat{\mathbf{g}} &= \mathbb{E}_{\mathbf{x} \in \mathcal{X}} [Q(\hat{\mathbf{z}}, \mathbf{J}_t)(\mathbf{z}_t - \hat{\mathbf{z}})] + \mathbb{E}_{\mathbf{x} \in \mathcal{X}} [Q_t^{21}(\hat{\mathbf{z}})] + \mathbb{E}_{\mathbf{x} \in \mathcal{X}} [\mathbf{J}_t Q_t^{\text{ls-11}}(\hat{\mathbf{z}})] \end{aligned} \tag{25}$$

where

$$\begin{aligned} Q_t^{21}(\mathbf{z}) &\triangleq \nabla_2 \mathcal{L}_{\mathbf{x}}(\mathbf{z}_t, \mathbf{D}) - \nabla_2 \mathcal{L}_{\mathbf{x}}(\mathbf{z}, \mathbf{D}) - \nabla_{21}^2 \mathcal{L}_{\mathbf{x}}(\mathbf{z}, \mathbf{D})(\mathbf{z}_t - \mathbf{z}) \\ Q_t^{\text{lasso-11}}(\mathbf{z}) &\triangleq \nabla_1 \mathcal{L}_{\mathbf{x}}(\mathbf{z}_t, \mathbf{D}) + \partial h(\mathbf{z}_t) - \nabla_{11}^2 \mathcal{L}_{\mathbf{x}}(\mathbf{z}, \mathbf{D})(\mathbf{z}_t - \mathbf{z}) \\ Q_t^{\text{ls-11}}(\mathbf{z}) &\triangleq \nabla_1 \mathcal{L}_{\mathbf{x}}(\mathbf{z}_t, \mathbf{D}) - \nabla_{11}^2 \mathcal{L}_{\mathbf{x}}(\mathbf{z}, \mathbf{D})(\mathbf{z}_t - \mathbf{z}) \\ Q(\mathbf{z}, \mathbf{J}) &\triangleq \mathbf{J} \nabla_{11}^2 \mathcal{L}_{\mathbf{x}}(\mathbf{z}, \mathbf{D}) + \nabla_{21}^2 \mathcal{L}_{\mathbf{x}}(\mathbf{z}, \mathbf{D}). \end{aligned} \tag{26}$$

Hence, it suffices to bound the terms on the *r.h.s.* Given [Assumption 3.1](#) and [Lemma 3.1](#),

$$\|\mathbf{g}_t^{\text{ae-lasso}} - \hat{\mathbf{g}}\|_2 \leq \mathbb{E}_{\mathbf{x} \in \mathcal{X}} [L_1 \|\mathbf{J}_t - \hat{\mathbf{J}}\|_2 \|\mathbf{z}_t - \hat{\mathbf{z}}\|_2 + (L_{21}/2) \|\mathbf{z}_t - \hat{\mathbf{z}}\|_2^2 + M_J (L_{11}/2) \|\mathbf{z}_t - \hat{\mathbf{z}}\|_2^2]. \tag{27}$$

Using the convergence errors from the forward pass ([Theorems 3.1 and 3.2](#)),

$$\|\mathbf{g}_t^{\text{ae-lasso}} - \hat{\mathbf{g}}\|_2 \leq L_1 O(t\rho^{2t-1}) + (L_{21}/2 + M_J (L_{11}/2)) O(\rho^{2t}) = O(t\rho^{2t-1}). \tag{28}$$

Similarly,

$$\|\mathbf{g}_t^{\text{ae-ls}} - \hat{\mathbf{g}}\|_2 \leq \mathbb{E}_{\mathbf{x} \in \mathcal{X}} [L_1 \|\mathbf{J}_t - \hat{\mathbf{J}}\|_2 \|\mathbf{z}_t - \hat{\mathbf{z}}\|_2 + (L_{21}/2) \|\mathbf{z}_t - \hat{\mathbf{z}}\|_2^2 + M_J ((L_{11}/2) \|\mathbf{z}_t - \hat{\mathbf{z}}\|_2^2 + \|\partial h(\hat{\mathbf{z}})\|_2)]. \tag{29}$$

Using the convergence errors from the forward pass ([Theorems 3.1 and 3.2](#)),

$$\|\mathbf{g}_t^{\text{ae-ls}} - \hat{\mathbf{g}}\|_2 \leq L_1 O(t\rho^{2t-1}) + (L_{21}/2 + M_J L_{11}/2) O(\rho^{2t}) + M_J \|\partial h(\hat{\mathbf{z}})\|_2 = O(t\rho^{2t-1} + \hat{C}_h). \tag{30}$$

■

A.4 Proof of Lemma 3.1

Lemma 3.1 (Local bounds). *From local gradient errors in Theorem 3.3, the following are satisfied*

$$\begin{aligned} \|Q_t^{21}(\hat{\mathbf{z}})\|_2 &\leq (L_{21}/2)\|\mathbf{z}_t - \hat{\mathbf{z}}\|_2^2, & \|Q_t^{\text{lasso-11}}(\hat{\mathbf{z}})\|_2 &\leq (L_{11}/2)\|\mathbf{z}_t - \hat{\mathbf{z}}\|_2^2 \\ \|Q(\hat{\mathbf{z}}, \mathbf{J}_t)\|_2 &\leq L_1\|\mathbf{J}_t - \hat{\mathbf{J}}\|_2, & \|Q_t^{\text{ls-11}}(\hat{\mathbf{z}})\|_2 &\leq (L_{11}/2)\|\mathbf{z}_t - \hat{\mathbf{z}}\|_2^2 + \|\partial h(\hat{\mathbf{z}})\|_2. \end{aligned} \quad (14)$$

Proof. For $Q_t^{21}(\hat{\mathbf{z}})$, given convexity of $\nabla_1 \mathcal{L}_{\mathbf{x}}(\mathbf{z}, \mathbf{D})$ and its domain (Assumption 2.1) and Lemma 2.2, we achieve the quadratic upper bound. For $Q_t^{\text{lasso-11}}(\hat{\mathbf{z}})$, we add and subtract $\nabla_1 \mathcal{L}_{\mathbf{x}}(\hat{\mathbf{z}}, \mathbf{D})$, and then use quadratic upper bound. At line four, given Lemma A.3, we use $\mathbf{0} \in \nabla_1 \mathcal{L}_{\mathbf{x}}(\hat{\mathbf{z}}, \mathbf{D}) + \partial h(\hat{\mathbf{z}})$ and assume that \mathbf{z}_t recovers the sign entries of $\hat{\mathbf{z}}$.

$$\begin{aligned} \|Q_t^{\text{lasso-11}}\|_2 &= \|\nabla_1 \mathcal{L}_{\mathbf{x}}(\mathbf{z}_t, \mathbf{D}) + \partial h(\mathbf{z}_t) - \nabla_{11}^2 \mathcal{L}_{\mathbf{x}}(\hat{\mathbf{z}}, \mathbf{D})(\mathbf{z}_t - \hat{\mathbf{z}})\| \\ &= \|\nabla_1 \mathcal{L}_{\mathbf{x}}(\mathbf{z}_t, \mathbf{D}) - \nabla_1 \mathcal{L}_{\mathbf{x}}(\hat{\mathbf{z}}, \mathbf{D}) + \nabla_1 \mathcal{L}_{\mathbf{x}}(\hat{\mathbf{z}}, \mathbf{D}) + \partial h(\mathbf{z}_t) - \nabla_{11}^2 \mathcal{L}_{\mathbf{x}}(\hat{\mathbf{z}}, \mathbf{D})(\mathbf{z}_t - \hat{\mathbf{z}})\| \\ &\leq (L_{11}/2)\|\mathbf{z}_t - \hat{\mathbf{z}}\|_2^2 + \|\partial h(\mathbf{z}_t) + \nabla_1 \mathcal{L}_{\mathbf{x}}(\hat{\mathbf{z}}, \mathbf{D})\|_2 \\ &\in (L_{11}/2)\|\mathbf{z}_t - \hat{\mathbf{z}}\|_2^2 + \|\partial h(\mathbf{z}_t) - \partial h(\hat{\mathbf{z}})\|_2 \\ &\leq (L_{11}/2)\|\mathbf{z}_t - \hat{\mathbf{z}}\|_2^2. \end{aligned} \quad (31)$$

Similarly,

$$\begin{aligned} \|Q_t^{\text{ls-11}}\|_2 &= \|\nabla_1 \mathcal{L}_{\mathbf{x}}(\mathbf{z}_t, \mathbf{D}) - \nabla_{11}^2 \mathcal{L}_{\mathbf{x}}(\hat{\mathbf{z}}, \mathbf{D})(\mathbf{z}_t - \hat{\mathbf{z}})\| \\ &= \|\nabla_1 \mathcal{L}_{\mathbf{x}}(\mathbf{z}_t, \mathbf{D}) - \nabla_1 \mathcal{L}_{\mathbf{x}}(\hat{\mathbf{z}}, \mathbf{D}) + \nabla_1 \mathcal{L}_{\mathbf{x}}(\hat{\mathbf{z}}, \mathbf{D}) - \nabla_{11}^2 \mathcal{L}_{\mathbf{x}}(\hat{\mathbf{z}}, \mathbf{D})(\mathbf{z}_t - \hat{\mathbf{z}})\| \\ &\leq (L_{11}/2)\|\mathbf{z}_t - \hat{\mathbf{z}}\|_2^2 + \|\nabla_1 \mathcal{L}_{\mathbf{x}}(\hat{\mathbf{z}}, \mathbf{D})\|_2 \in (L_{11}/2)\|\mathbf{z}_t - \hat{\mathbf{z}}\|_2^2 + \|\partial h(\hat{\mathbf{z}})\|_2. \end{aligned} \quad (32)$$

For $Q(\hat{\mathbf{z}}, \mathbf{J}_t)$, from implicit function theorem, $Q(\hat{\mathbf{z}}, \hat{\mathbf{J}}) = 0$. Hence, we can use $\nabla_{21}^2 \mathcal{L}_{\mathbf{x}}(\hat{\mathbf{z}}, \mathbf{D}) = -\hat{\mathbf{J}} \nabla_{11}^2 \mathcal{L}_{\mathbf{x}}(\hat{\mathbf{z}}, \mathbf{D})$ in the following

$$\begin{aligned} \|Q(\hat{\mathbf{z}}, \mathbf{J}_t)\|_2 &= \|\mathbf{J}_t \nabla_{11}^2 \mathcal{L}_{\mathbf{x}}(\hat{\mathbf{z}}, \mathbf{D}) + \nabla_{21}^2 \mathcal{L}_{\mathbf{x}}(\hat{\mathbf{z}}, \mathbf{D})\|_2 \\ &= \|\mathbf{J}_t \nabla_{11}^2 \mathcal{L}_{\mathbf{x}}(\hat{\mathbf{z}}, \mathbf{D}) - \hat{\mathbf{J}} \nabla_{11}^2 \mathcal{L}_{\mathbf{x}}(\hat{\mathbf{z}}, \mathbf{D})\|_2 \\ &\leq \|(\mathbf{J}_t - \hat{\mathbf{J}}) \nabla_{11}^2 \mathcal{L}_{\mathbf{x}}(\hat{\mathbf{z}}, \mathbf{D})\|_2 \leq L_1 \|\mathbf{J}_t - \hat{\mathbf{J}}\|_2. \end{aligned} \quad (33)$$

■

A.5 Proof of Theorem 3.4

Theorem 3.4 (Global convergence of gradients). *Given the convergence results from the forward pass, (Theorems 3.1 and 3.2), $\exists \rho < 1, B > 0$ such that $\forall t > B$, the errors of gradients defined in Algorithm 2 w.r.t global directions \mathbf{g}^* and $\tilde{\mathbf{g}}$ (defined in (6)) satisfy*

$$\begin{aligned} \|\mathbf{g}_t^{\text{dec}} - \mathbf{g}^*\|_2 &\leq O(\rho^t + C_z^*) \\ \|\mathbf{g}_t^{\text{ae-lasso}} - \mathbf{g}^*\|_2 &\leq O(t\rho^{2t-1} + C_z^* t\rho^{t-1} + \rho^t C_J^* + (C_z^* + 1)C_J^* + C_D^*) \end{aligned} \quad (15)$$

$$\|\mathbf{g}_t^{\text{ae-ls}} - \mathbf{g}^*\|_2 \leq O(t\rho^{2t-1} + C_z^* t\rho^{t-1} + \rho^t C_J^* + (C_z^* + 1)C_J^* + C_D^* + C_h^*)$$

$$\|\mathbf{g}_t^{\text{dec}} - \tilde{\mathbf{g}}\|_2 \leq O(\rho^t + \tilde{C}_z)$$

$$\|\mathbf{g}_t^{\text{ae-lasso}} - \tilde{\mathbf{g}}\|_2 \leq O(t\rho^{2t-1} + \tilde{C}_z t\rho^{t-1} + \rho^t \tilde{C}_J + (\tilde{C}_z + 1)\tilde{C}_J + \tilde{C}_D + C_h^t) \quad (16)$$

$$\|\mathbf{g}_t^{\text{ae-ls}} - \tilde{\mathbf{g}}\|_2 \leq O(t\rho^{2t-1} + \tilde{C}_z t\rho^{t-1} + \rho^t \tilde{C}_J + (\tilde{C}_z + 1)\tilde{C}_J + \tilde{C}_D)$$

where $C_z^* \triangleq O(\|\hat{\mathbf{z}} - \mathbf{z}^*\|_2)$, $C_J^* \triangleq O(\|\hat{\mathbf{J}} - \mathbf{J}^*\|_2)$, $C_D^* \triangleq O(\|\mathbf{D} - \mathbf{D}^*\|_2)$, and C_h^* is an upper bound on $M_J \|\partial h(\mathbf{z}^*)\|_2$. Similarly, we have $\tilde{C}_z \triangleq O(\|\hat{\mathbf{z}} - \tilde{\mathbf{z}}\|_2)$, $\tilde{C}_J^* \triangleq O(\|\hat{\mathbf{J}} - \tilde{\mathbf{J}}\|_2)$, $\tilde{C}_D^* \triangleq O(\|\mathbf{D} - \tilde{\mathbf{D}}\|_2)$, and C_h^t is an upper bound on $M_J \|\partial h(\mathbf{z}_t)\|_2$.

Proof. For $\mathbf{g}_t^{\text{dec}}$, we compute the gradient in their limit assuming infinite fresh samples $\lim_{n \rightarrow \infty} \frac{1}{n} \sum_{i=1}^n \nabla_2 \mathcal{L}_{\mathbf{x}^i}(\mathbf{z}_t^i, \mathbf{D}) = \mathbb{E}_{\mathbf{x} \in \mathcal{X}} [\nabla_2 \mathcal{L}_{\mathbf{x}}(\mathbf{z}_t, \mathbf{D})]$ a.s.. Based on Lemma 2.2,

$$\begin{aligned} \|\mathbf{g}_t^{\text{dec}} - \mathbf{g}^*\|_2 &= \|\mathbb{E}_{\mathbf{x} \in \mathcal{X}} [\nabla_2 \mathcal{L}_{\mathbf{x}}(\mathbf{z}_t, \mathbf{D})] - \mathbb{E}_{\mathbf{x} \in \mathcal{X}} [\nabla_2 \mathcal{L}_{\mathbf{x}}(\mathbf{z}^*, \mathbf{D})]\|_2 \\ &\leq \mathbb{E}_{\mathbf{x} \in \mathcal{X}} [\|\nabla_2 \mathcal{L}_{\mathbf{x}}(\mathbf{z}_t, \mathbf{D}) - \nabla_2 \mathcal{L}_{\mathbf{x}}(\mathbf{z}^*, \mathbf{D})\|_2] \\ &\leq \mathbb{E}_{\mathbf{x} \in \mathcal{X}} [L_2 \|\mathbf{z}_t - \mathbf{z}^*\|_2] \\ &\leq O(\rho^t + C_z^*). \end{aligned} \quad (34)$$

Similar to [Theorem 3.3](#), we re-write the errors of gradients $\mathbf{g}_t^{\text{ae-lasso}}$ and $\mathbf{g}_t^{\text{ae-ls}}$ as following

$$\begin{aligned}\mathbf{g}_t^{\text{ae-lasso}} - \mathbf{g}^* &= \mathbb{E}_{\mathbf{x} \in \mathcal{X}} [Q(\mathbf{z}^*, \mathbf{J}_t)(\mathbf{z}_t - \mathbf{z}^*)] + \mathbb{E}_{\mathbf{x} \in \mathcal{X}} [Q_t^{21}(\mathbf{z}^*)] + \mathbb{E}_{\mathbf{x} \in \mathcal{X}} [\mathbf{J}_t Q_t^{\text{lasso-11}}(\mathbf{z}^*)] \\ \mathbf{g}_t^{\text{ae-ls}} - \mathbf{g}^* &= \mathbb{E}_{\mathbf{x} \in \mathcal{X}} [Q(\mathbf{z}^*, \mathbf{J}_t)(\mathbf{z}_t - \mathbf{z}^*)] + \mathbb{E}_{\mathbf{x} \in \mathcal{X}} [Q_t^{21}(\mathbf{z}^*)] + \mathbb{E}_{\mathbf{x} \in \mathcal{X}} [\mathbf{J}_t Q_t^{\text{ls-11}}(\mathbf{z}^*)]\end{aligned}\quad (35)$$

and

$$\begin{aligned}\mathbf{g}_t^{\text{ae-lasso}} - \tilde{\mathbf{g}} &= \mathbb{E}_{\mathbf{x} \in \mathcal{X}} [Q(\tilde{\mathbf{z}}, \mathbf{J}_t)(\mathbf{z}_t - \tilde{\mathbf{z}})] + \mathbb{E}_{\mathbf{x} \in \mathcal{X}} [Q_t^{21}(\tilde{\mathbf{z}})] + \mathbb{E}_{\mathbf{x} \in \mathcal{X}} [\mathbf{J}_t Q_t^{\text{lasso-11}}(\tilde{\mathbf{z}})] \\ \mathbf{g}_t^{\text{ae-ls}} - \tilde{\mathbf{g}} &= \mathbb{E}_{\mathbf{x} \in \mathcal{X}} [Q(\tilde{\mathbf{z}}, \mathbf{J}_t)(\mathbf{z}_t - \tilde{\mathbf{z}})] + \mathbb{E}_{\mathbf{x} \in \mathcal{X}} [Q_t^{21}(\tilde{\mathbf{z}})] + \mathbb{E}_{\mathbf{x} \in \mathcal{X}} [\mathbf{J}_t Q_t^{\text{ls-11}}(\tilde{\mathbf{z}})].\end{aligned}\quad (36)$$

where $Q_t^{21}(\mathbf{z})$, $Q_t^{\text{lasso-11}}(\mathbf{z})$, $Q_t^{\text{ls-11}}(\mathbf{z})$, and $Q(\mathbf{z}, \mathbf{J})$ are defined as in [Theorem 3.3](#). Given [Assumption 3.1](#) and [Lemma 3.2](#), we find an upper bound on *r.h.s.*

$$\begin{aligned}\|\mathbf{g}_t^{\text{ae-lasso}} - \mathbf{g}^*\|_2 &\leq \mathbb{E}_{\mathbf{x} \in \mathcal{X}} [L_1 \|\mathbf{J}_t - \mathbf{J}^*\|_2 \|\mathbf{z}_t - \mathbf{z}^*\|_2 + (L_{21}/2) \|\mathbf{z}_t - \mathbf{z}^*\|_2^2] \\ &\quad + \mathbb{E}_{\mathbf{x} \in \mathcal{X}} [M_J (L_{11}/2) \|\mathbf{z}_t - \mathbf{z}^*\|_2^2 + L_D \|\mathbf{D} - \mathbf{D}^*\|_2] \\ &\leq \mathbb{E}_{\mathbf{x} \in \mathcal{X}} [L_1 (\|\mathbf{J}_t - \hat{\mathbf{J}}\|_2 + \|\hat{\mathbf{J}} - \mathbf{J}^*\|_2) (\|\mathbf{z}_t - \hat{\mathbf{z}}\|_2 + \|\hat{\mathbf{z}} - \mathbf{z}^*\|_2)] \\ &\quad + \mathbb{E}_{\mathbf{x} \in \mathcal{X}} [(L_{21}/2) (\|\mathbf{z}_t - \hat{\mathbf{z}}\|_2^2 + \|\hat{\mathbf{z}} - \mathbf{z}^*\|_2^2)] \\ &\quad + \mathbb{E}_{\mathbf{x} \in \mathcal{X}} [M_J (L_{11}/2) (\|\mathbf{z}_t - \hat{\mathbf{z}}\|_2^2 + \|\hat{\mathbf{z}} - \mathbf{z}^*\|_2^2) + L_D \|\mathbf{D} - \mathbf{D}^*\|_2].\end{aligned}\quad (37)$$

Similarly,

$$\begin{aligned}\|\mathbf{g}_t^{\text{ae-ls}} - \mathbf{g}^*\|_2 &\leq \mathbb{E}_{\mathbf{x} \in \mathcal{X}} [L_1 \|\mathbf{J}_t - \mathbf{J}^*\|_2 \|\mathbf{z}_t - \mathbf{z}^*\|_2 + (L_{21}/2) \|\mathbf{z}_t - \mathbf{z}^*\|_2^2] \\ &\quad + \mathbb{E}_{\mathbf{x} \in \mathcal{X}} [M_J (L_{11}/2) \|\mathbf{z}_t - \mathbf{z}^*\|_2^2 + M_J \|\partial h(\mathbf{z}^*)\|_2 + L_D \|\mathbf{D} - \mathbf{D}^*\|_2] \\ &\leq \mathbb{E}_{\mathbf{x} \in \mathcal{X}} [L_1 (\|\mathbf{J}_t - \hat{\mathbf{J}}\|_2 + \|\hat{\mathbf{J}} - \mathbf{J}^*\|_2) (\|\mathbf{z}_t - \hat{\mathbf{z}}\|_2 + \|\hat{\mathbf{z}} - \mathbf{z}^*\|_2)] \\ &\quad + \mathbb{E}_{\mathbf{x} \in \mathcal{X}} [(L_{21}/2) (\|\mathbf{z}_t - \hat{\mathbf{z}}\|_2^2 + \|\hat{\mathbf{z}} - \mathbf{z}^*\|_2^2) + L_D \|\mathbf{D} - \mathbf{D}^*\|_2] \\ &\quad + \mathbb{E}_{\mathbf{x} \in \mathcal{X}} [M_J (L_{11}/2) (\|\mathbf{z}_t - \hat{\mathbf{z}}\|_2^2 + \|\hat{\mathbf{z}} - \mathbf{z}^*\|_2^2) + M_J \|\partial h(\mathbf{z}^*)\|_2].\end{aligned}\quad (38)$$

Using the convergence errors from the forward pass ([Theorems 3.1](#) and [3.2](#)),

$$\begin{aligned}\|\mathbf{g}_t^{\text{ae-lasso}} - \mathbf{g}^*\|_2 &\leq L_1 (O(t\rho^{2t-1} + C_z^* t\rho^{t-1} + \rho^t C_J^* + C_z^* C_J^*)) \\ &\quad + (L_{21}/2 + M_J (L_{11}/2)) O(\rho^{2t} + C_z^*) + C_D^* \\ &= O(t\rho^{2t-1} + C_z^* t\rho^{t-1} + \rho^t C_J^* + (C_z^* + 1)C_J^* + C_D^*)\end{aligned}\quad (39)$$

and

$$\begin{aligned}\|\mathbf{g}_t^{\text{ae-ls}} - \mathbf{g}^*\|_2 &\leq L_1 (O(t\rho^{2t-1} + C_z^* t\rho^{t-1} + \rho^t C_J^* + C_z^* C_J^*)) \\ &\quad + (L_{21}/2 + M_J L_{11}/2) O(\rho^{2t} + C_z^*) + C_D^* + M_J \|\partial h(\mathbf{z}^*)\|_2 \\ &= O(t\rho^{2t-1} + C_z^* t\rho^{t-1} + \rho^t C_J^* + (C_z^* + 1)C_J^* + C_D^*) \\ &\leq L_1 O(t\rho^{2t-1}) + (L_{21}/2 + M_J L_{11}/2) O(\rho^{2t}) + C_h^* \\ &= O(t\rho^{2t-1} + C_z^* t\rho^{t-1} + \rho^t C_J^* + (C_z^* + 1)C_J^* + C_D^* + C_h^*).\end{aligned}\quad (40)$$

The steps to bound the errors w.r.t $\tilde{\mathbf{g}}$ is similar. We have

$$\begin{aligned}\|\mathbf{g}_t^{\text{ae-lasso}} - \tilde{\mathbf{g}}\|_2 &\leq \mathbb{E}_{\mathbf{x} \in \mathcal{X}} [L_1 \|\mathbf{J}_t - \tilde{\mathbf{J}}\|_2 \|\mathbf{z}_t - \tilde{\mathbf{z}}\|_2 + (L_{21}/2) \|\mathbf{z}_t - \tilde{\mathbf{z}}\|_2^2] \\ &\quad + \mathbb{E}_{\mathbf{x} \in \mathcal{X}} [M_J (L_{11}/2) \|\mathbf{z}_t - \tilde{\mathbf{z}}\|_2^2 + M_J \|\partial h(\mathbf{z}_t)\|_2 + L_D \|\mathbf{D} - \tilde{\mathbf{D}}\|_2] \\ &\leq \mathbb{E}_{\mathbf{x} \in \mathcal{X}} [L_1 (\|\mathbf{J}_t - \hat{\mathbf{J}}\|_2 + \|\hat{\mathbf{J}} - \tilde{\mathbf{J}}\|_2) (\|\mathbf{z}_t - \hat{\mathbf{z}}\|_2 + \|\hat{\mathbf{z}} - \tilde{\mathbf{z}}\|_2)] \\ &\quad + \mathbb{E}_{\mathbf{x} \in \mathcal{X}} [(L_{21}/2) (\|\mathbf{z}_t - \hat{\mathbf{z}}\|_2^2 + \|\hat{\mathbf{z}} - \tilde{\mathbf{z}}\|_2^2) + L_D \|\mathbf{D} - \tilde{\mathbf{D}}\|_2] \\ &\quad + \mathbb{E}_{\mathbf{x} \in \mathcal{X}} [M_J (L_{11}/2) (\|\mathbf{z}_t - \hat{\mathbf{z}}\|_2^2 + \|\hat{\mathbf{z}} - \tilde{\mathbf{z}}\|_2^2) + M_J \|\partial h(\mathbf{z}_t)\|_2]\end{aligned}\quad (41)$$

and

$$\begin{aligned}\|\mathbf{g}_t^{\text{ae-ls}} - \tilde{\mathbf{g}}\|_2 &\leq \mathbb{E}_{\mathbf{x} \in \mathcal{X}} [L_1 \|\mathbf{J}_t - \tilde{\mathbf{J}}\|_2 \|\mathbf{z}_t - \tilde{\mathbf{z}}\|_2 + (L_{21}/2) \|\mathbf{z}_t - \tilde{\mathbf{z}}\|_2^2] \\ &\quad + \mathbb{E}_{\mathbf{x} \in \mathcal{X}} [M_J (L_{11}/2) \|\mathbf{z}_t - \tilde{\mathbf{z}}\|_2^2 + L_D \|\mathbf{D} - \tilde{\mathbf{D}}\|_2] \\ &\leq \mathbb{E}_{\mathbf{x} \in \mathcal{X}} [L_1 (\|\mathbf{J}_t - \hat{\mathbf{J}}\|_2 + \|\hat{\mathbf{J}} - \tilde{\mathbf{J}}\|_2) (\|\mathbf{z}_t - \hat{\mathbf{z}}\|_2 + \|\hat{\mathbf{z}} - \tilde{\mathbf{z}}\|_2)] \\ &\quad + \mathbb{E}_{\mathbf{x} \in \mathcal{X}} [(L_{21}/2) (\|\mathbf{z}_t - \hat{\mathbf{z}}\|_2^2 + \|\hat{\mathbf{z}} - \tilde{\mathbf{z}}\|_2^2)] \\ &\quad + \mathbb{E}_{\mathbf{x} \in \mathcal{X}} [M_J (L_{11}/2) (\|\mathbf{z}_t - \hat{\mathbf{z}}\|_2^2 + \|\hat{\mathbf{z}} - \tilde{\mathbf{z}}\|_2^2) + L_D \|\mathbf{D} - \tilde{\mathbf{D}}\|_2].\end{aligned}\quad (42)$$

From convergence rates in the forward pass ([Theorems 3.1 and 3.2](#)), we get

$$\begin{aligned}
\|\mathbf{g}_t^{\text{ae-lasso}} - \tilde{\mathbf{g}}\|_2 &\leq L_1 \left(O(t\rho^{2t-1} + \tilde{C}_z t\rho^{t-1} + \rho^t \tilde{C}_J + \tilde{C}_z \tilde{C}_J) \right) \\
&\quad + (L_{21}/2 + M_J L_{11}/2) O(\rho^{2t} + \tilde{C}_z) + \tilde{C}_D + M_J \|\partial h(\mathbf{z}_t)\|_2 \\
&= O(t\rho^{2t-1} + \tilde{C}_z t\rho^{t-1} + \rho^t \tilde{C}_J + (\tilde{C}_z + 1)\tilde{C}_J + \tilde{C}_D) \\
&\leq L_1 O(t\rho^{2t-1}) + (L_{21}/2 + M_J L_{11}/2) O(\rho^{2t}) + C_h^t \\
&= O(t\rho^{2t-1} + \tilde{C}_z t\rho^{t-1} + \rho^t \tilde{C}_J + (\tilde{C}_z + 1)\tilde{C}_J + \tilde{C}_D + C_h^t)
\end{aligned} \tag{43}$$

and

$$\begin{aligned}
\|\mathbf{g}_t^{\text{ae-ls}} - \tilde{\mathbf{g}}\|_2 &\leq L_1 \left(O(t\rho^{2t-1} + \tilde{C}_z t\rho^{t-1} + \rho^t \tilde{C}_J + \tilde{C}_z \tilde{C}_J) \right) \\
&\quad + (L_{21}/2 + M_J L_{11}/2) O(\rho^{2t} + \tilde{C}_z) + \tilde{C}_D \\
&= O(t\rho^{2t-1} + \tilde{C}_z t\rho^{t-1} + \rho^t \tilde{C}_J + (\tilde{C}_z + 1)\tilde{C}_J + \tilde{C}_D).
\end{aligned} \tag{44}$$

■

A.6 Proof of [Lemma 3.2](#)

Lemma 3.2 (Global bounds). *From global gradient errors in [Theorem 3.4](#), the following are satisfied*

$$\begin{aligned}
\|Q_t^{21}(\mathbf{z}^*)\|_2 &\leq (L_{21}/2)\|\mathbf{z}_t - \mathbf{z}^*\|_2^2 \\
\|Q_t^{\text{lasso-11}}(\mathbf{z}^*)\|_2 &\leq (L_{11}/2)\|\mathbf{z}_t - \mathbf{z}^*\|_2^2 + L_D\|\mathbf{D} - \mathbf{D}^*\|_2 \\
\|Q_t^{\text{ls-11}}(\mathbf{z}^*)\|_2 &\leq (L_{11}/2)\|\mathbf{z}_t - \mathbf{z}^*\|_2^2 + L_D\|\mathbf{D} - \mathbf{D}^*\|_2 + \|\partial h(\mathbf{z}^*)\|_2 \\
\|Q(\mathbf{z}^*, \mathbf{J}_t)\|_2 &\leq L_1\|\mathbf{J}_t - \mathbf{J}^*\|_2
\end{aligned} \tag{20}$$

$$\begin{aligned}
\|Q_t^{21}(\tilde{\mathbf{z}})\|_2 &\leq (L_{21}/2)\|\mathbf{z}_t - \tilde{\mathbf{z}}\|_2^2 \\
\|Q_t^{\text{lasso-11}}(\tilde{\mathbf{z}})\|_2 &\leq (L_{11}/2)\|\mathbf{z}_t - \tilde{\mathbf{z}}\|_2^2 + L_D\|\mathbf{D} - \tilde{\mathbf{D}}\|_2 + \|\partial h(\mathbf{z}_t)\|_2 \\
\|Q_t^{\text{ls-11}}(\tilde{\mathbf{z}})\|_2 &\leq (L_{11}/2)\|\mathbf{z}_t - \tilde{\mathbf{z}}\|_2^2 + L_D\|\mathbf{D} - \tilde{\mathbf{D}}\|_2 \\
\|Q(\tilde{\mathbf{z}}, \mathbf{J}_t)\|_2 &\leq L_1\|\mathbf{J}_t - \tilde{\mathbf{J}}\|_2.
\end{aligned} \tag{21}$$

Proof. For $Q_t^{21}(\mathbf{z}^*)$ and $Q_t^{21}(\tilde{\mathbf{z}})$, we achieve the quadratic bound using convexity of $\nabla_1 \mathcal{L}_{\mathbf{x}}(\mathbf{z}, \mathbf{D})$ and its domain ([Assumption 2.1](#)) and [Lemma 2.2](#). For $Q_t^{\text{lasso-11}}(\mathbf{z}^*)$, we add and subtract $\nabla_1 \mathcal{L}_{\mathbf{x}}(\mathbf{z}^*, \mathbf{D})$ and $\nabla_1 \mathcal{L}_{\mathbf{x}}(\mathbf{z}^*, \mathbf{D}^*)$, and use quadratic upper bound similar to [Lemma 3.1](#). At line five, we use $\mathbf{0} \in \nabla_1 \mathcal{L}_{\mathbf{x}}(\mathbf{z}^*, \mathbf{D}^*) + \partial h(\mathbf{z}^*)$ ([Lemma A.3](#)) and assume that \mathbf{z}_t recovers the sign entries of \mathbf{z}^* .

$$\begin{aligned}
\|Q_t^{\text{lasso-11}}(\mathbf{z}^*)\|_2 &= \|\nabla_1 \mathcal{L}_{\mathbf{x}}(\mathbf{z}_t, \mathbf{D}) + \partial h(\mathbf{z}_t) - \nabla_{11}^2 \mathcal{L}_{\mathbf{x}}(\mathbf{z}^*, \mathbf{D})(\mathbf{z}_t - \mathbf{z}^*)\|_2 \\
&= \|\nabla_1 \mathcal{L}_{\mathbf{x}}(\mathbf{z}_t, \mathbf{D}) - \nabla_1 \mathcal{L}_{\mathbf{x}}(\mathbf{z}^*, \mathbf{D}) + \nabla_1 \mathcal{L}_{\mathbf{x}}(\mathbf{z}^*, \mathbf{D}) + \partial h(\mathbf{z}_t) - \nabla_{11}^2 \mathcal{L}_{\mathbf{x}}(\mathbf{z}^*, \mathbf{D})(\mathbf{z}_t - \mathbf{z}^*)\|_2 \\
&\leq (L_{11}/2)\|\mathbf{z}_t - \mathbf{z}^*\|_2^2 + \|\partial h(\mathbf{z}_t) + \nabla_1 \mathcal{L}_{\mathbf{x}}(\mathbf{z}^*, \mathbf{D})\|_2 \\
&\leq (L_{11}/2)\|\mathbf{z}_t - \mathbf{z}^*\|_2^2 + \|\partial h(\mathbf{z}_t) + \nabla_1 \mathcal{L}_{\mathbf{x}}(\mathbf{z}^*, \mathbf{D}) - \nabla_1 \mathcal{L}_{\mathbf{x}}(\mathbf{z}^*, \mathbf{D}^*) + \nabla_1 \mathcal{L}_{\mathbf{x}}(\mathbf{z}^*, \mathbf{D}^*)\|_2 \\
&\leq (L_{11}/2)\|\mathbf{z}_t - \mathbf{z}^*\|_2^2 + L_D\|\mathbf{D} - \mathbf{D}^*\|_2 + \|\partial h(\mathbf{z}_t) + \nabla_1 \mathcal{L}_{\mathbf{x}}(\mathbf{z}^*, \mathbf{D}^*)\|_2 \\
&\in (L_{11}/2)\|\mathbf{z}_t - \mathbf{z}^*\|_2^2 + L_D\|\mathbf{D} - \mathbf{D}^*\|_2 + \|\partial h(\mathbf{z}_t) - \partial h(\mathbf{z}^*)\|_2 \\
&\leq (L_{11}/2)\|\mathbf{z}_t - \mathbf{z}^*\|_2^2 + L_D\|\mathbf{D} - \mathbf{D}^*\|_2.
\end{aligned} \tag{45}$$

Similarly,

$$\begin{aligned}
\|Q_t^{\text{ls-11}}(\mathbf{z}^*)\|_2 &= \|\nabla_1 \mathcal{L}_{\mathbf{x}}(\mathbf{z}_t, \mathbf{D}) - \nabla_{11}^2 \mathcal{L}_{\mathbf{x}}(\mathbf{z}^*, \mathbf{D})(\mathbf{z}_t - \mathbf{z}^*)\|_2 \\
&= \|\nabla_1 \mathcal{L}_{\mathbf{x}}(\mathbf{z}_t, \mathbf{D}) - \nabla_1 \mathcal{L}_{\mathbf{x}}(\mathbf{z}^*, \mathbf{D}) + \nabla_1 \mathcal{L}_{\mathbf{x}}(\mathbf{z}^*, \mathbf{D}) - \nabla_{11}^2 \mathcal{L}_{\mathbf{x}}(\mathbf{z}^*, \mathbf{D})(\mathbf{z}_t - \mathbf{z}^*)\|_2 \\
&\leq (L_{11}/2)\|\mathbf{z}_t - \mathbf{z}^*\|_2^2 + \|\nabla_1 \mathcal{L}_{\mathbf{x}}(\mathbf{z}^*, \mathbf{D})\|_2 \\
&\leq (L_{11}/2)\|\mathbf{z}_t - \mathbf{z}^*\|_2^2 + \|\nabla_1 \mathcal{L}_{\mathbf{x}}(\mathbf{z}^*, \mathbf{D}) - \nabla_1 \mathcal{L}_{\mathbf{x}}(\mathbf{z}^*, \mathbf{D}^*) + \nabla_1 \mathcal{L}_{\mathbf{x}}(\mathbf{z}^*, \mathbf{D}^*)\|_2 \\
&\leq (L_{11}/2)\|\mathbf{z}_t - \mathbf{z}^*\|_2^2 + L_D\|\mathbf{D} - \mathbf{D}^*\|_2 + \|\nabla_1 \mathcal{L}_{\mathbf{x}}(\mathbf{z}^*, \mathbf{D}^*)\|_2 \\
&\in (L_{11}/2)\|\mathbf{z}_t - \mathbf{z}^*\|_2^2 + L_D\|\mathbf{D} - \mathbf{D}^*\|_2 + \|\partial h(\mathbf{z}^*)\|_2 \\
&\leq (L_{11}/2)\|\mathbf{z}_t - \mathbf{z}^*\|_2^2 + L_D\|\mathbf{D} - \mathbf{D}^*\|_2 + \|\partial h(\mathbf{z}^*)\|_2.
\end{aligned} \tag{46}$$

For $Q(\mathbf{z}^*, \mathbf{J}_t)$, from implicit function theorem, $Q(\mathbf{z}^*, \mathbf{J}^*) = 0$. Hence, we can use $\nabla_{21}^2 \mathcal{L}_{\mathbf{x}}(\mathbf{z}^*, \mathbf{D}) = -\mathbf{J}^* \nabla_{11}^2 \mathcal{L}_{\mathbf{x}}(\mathbf{z}^*, \mathbf{D})$ in the following

$$\begin{aligned} \|Q(\mathbf{z}^*, \mathbf{J}_t)\|_2 &= \|\mathbf{J}_t \nabla_{11}^2 \mathcal{L}_{\mathbf{x}}(\mathbf{z}^*, \mathbf{D}) + \nabla_{21}^2 \mathcal{L}_{\mathbf{x}}(\mathbf{z}^*, \mathbf{D})\|_2 \\ &= \|\mathbf{J}_t \nabla_{11}^2 \mathcal{L}_{\mathbf{x}}(\mathbf{z}^*, \mathbf{D}) - \mathbf{J}^* \nabla_{11}^2 \mathcal{L}_{\mathbf{x}}(\mathbf{z}^*, \mathbf{D})\|_2 \\ &\leq \|(\mathbf{J}_t - \mathbf{J}^*) \nabla_{11}^2 \mathcal{L}_{\mathbf{x}}(\mathbf{z}^*, \mathbf{D})\|_2 \leq L_1 \|\mathbf{J}_t - \mathbf{J}^*\|_2. \end{aligned} \quad (47)$$

For (21), the proof procedure is similar, where we instead use the property $\mathbf{0} = \nabla_1 \mathcal{L}_{\mathbf{x}}(\tilde{\mathbf{z}}, \tilde{\mathbf{D}})$.

$$\begin{aligned} \|Q_t^{\text{lasso-11}}(\tilde{\mathbf{z}})\|_2 &= \|\nabla_1 \mathcal{L}_{\mathbf{x}}(\mathbf{z}_t, \mathbf{D}) + \partial h(\mathbf{z}_t) - \nabla_{11}^2 \mathcal{L}_{\mathbf{x}}(\tilde{\mathbf{z}}, \mathbf{D})(\mathbf{z}_t - \tilde{\mathbf{z}})\|_2 \\ &= \|\nabla_1 \mathcal{L}_{\mathbf{x}}(\mathbf{z}_t, \mathbf{D}) - \nabla_1 \mathcal{L}_{\mathbf{x}}(\tilde{\mathbf{z}}, \mathbf{D}) + \nabla_1 \mathcal{L}_{\mathbf{x}}(\tilde{\mathbf{z}}, \mathbf{D}) + \partial h(\mathbf{z}_t) - \nabla_{11}^2 \mathcal{L}_{\mathbf{x}}(\tilde{\mathbf{z}}, \mathbf{D})(\mathbf{z}_t - \tilde{\mathbf{z}})\|_2 \\ &\leq (L_{11}/2) \|\mathbf{z}_t - \tilde{\mathbf{z}}\|_2^2 + \|\partial h(\mathbf{z}_t) + \nabla_1 \mathcal{L}_{\mathbf{x}}(\tilde{\mathbf{z}}, \mathbf{D})\|_2 \\ &\leq (L_{11}/2) \|\mathbf{z}_t - \tilde{\mathbf{z}}\|_2^2 + \|\partial h(\mathbf{z}_t) + \nabla_1 \mathcal{L}_{\mathbf{x}}(\tilde{\mathbf{z}}, \mathbf{D}) - \nabla_1 \mathcal{L}_{\mathbf{x}}(\tilde{\mathbf{z}}, \tilde{\mathbf{D}})\|_2 \\ &\leq (L_{11}/2) \|\mathbf{z}_t - \tilde{\mathbf{z}}\|_2^2 + L_D \|\mathbf{D} - \tilde{\mathbf{D}}\|_2 + \|\partial h(\mathbf{z}_t)\|_2. \end{aligned} \quad (48)$$

Similarly,

$$\begin{aligned} \|Q_t^{\text{ls-11}}(\tilde{\mathbf{z}})\|_2 &= \|\nabla_1 \mathcal{L}_{\mathbf{x}}(\mathbf{z}_t, \mathbf{D}) - \nabla_{11}^2 \mathcal{L}_{\mathbf{x}}(\tilde{\mathbf{z}}, \mathbf{D})(\mathbf{z}_t - \tilde{\mathbf{z}})\|_2 \\ &= \|\nabla_1 \mathcal{L}_{\mathbf{x}}(\mathbf{z}_t, \mathbf{D}) - \nabla_1 \mathcal{L}_{\mathbf{x}}(\tilde{\mathbf{z}}, \mathbf{D}) + \nabla_1 \mathcal{L}_{\mathbf{x}}(\tilde{\mathbf{z}}, \mathbf{D}) - \nabla_{11}^2 \mathcal{L}_{\mathbf{x}}(\tilde{\mathbf{z}}, \mathbf{D})(\mathbf{z}_t - \tilde{\mathbf{z}})\|_2 \\ &\leq (L_{11}/2) \|\mathbf{z}_t - \tilde{\mathbf{z}}\|_2^2 + \|\nabla_1 \mathcal{L}_{\mathbf{x}}(\tilde{\mathbf{z}}, \mathbf{D})\|_2 \\ &\leq (L_{11}/2) \|\mathbf{z}_t - \tilde{\mathbf{z}}\|_2^2 + \|\nabla_1 \mathcal{L}_{\mathbf{x}}(\tilde{\mathbf{z}}, \mathbf{D}) - \nabla_1 \mathcal{L}_{\mathbf{x}}(\tilde{\mathbf{z}}, \tilde{\mathbf{D}})\|_2 \\ &\leq (L_{11}/2) \|\mathbf{z}_t - \tilde{\mathbf{z}}\|_2^2 + L_D \|\mathbf{D} - \tilde{\mathbf{D}}\|_2. \end{aligned} \quad (49)$$

For $Q(\tilde{\mathbf{z}}, \mathbf{J}_t)$, from implicit function theorem, $Q(\tilde{\mathbf{z}}, \tilde{\mathbf{J}}) = 0$. Hence, we can use $\nabla_{21}^2 \mathcal{L}_{\mathbf{x}}(\tilde{\mathbf{z}}, \mathbf{D}) = -\tilde{\mathbf{J}} \nabla_{11}^2 \mathcal{L}_{\mathbf{x}}(\tilde{\mathbf{z}}, \mathbf{D})$ in the following

$$\begin{aligned} \|Q(\tilde{\mathbf{z}}, \mathbf{J}_t)\|_2 &= \|\mathbf{J}_t \nabla_{11}^2 \mathcal{L}_{\mathbf{x}}(\tilde{\mathbf{z}}, \mathbf{D}) + \nabla_{21}^2 \mathcal{L}_{\mathbf{x}}(\tilde{\mathbf{z}}, \mathbf{D})\|_2 \\ &= \|\mathbf{J}_t \nabla_{11}^2 \mathcal{L}_{\mathbf{x}}(\tilde{\mathbf{z}}, \mathbf{D}) - \tilde{\mathbf{J}} \nabla_{11}^2 \mathcal{L}_{\mathbf{x}}(\tilde{\mathbf{z}}, \mathbf{D})\|_2 \\ &\leq \|(\mathbf{J}_t - \tilde{\mathbf{J}}) \nabla_{11}^2 \mathcal{L}_{\mathbf{x}}(\tilde{\mathbf{z}}, \mathbf{D})\|_2 \leq L_1 \|\mathbf{J}_t - \tilde{\mathbf{J}}\|_2. \end{aligned} \quad (50)$$

■

B Details of experiments

PUDLE is developed using PyTorch [67] on Python. We used one GeForce GTX 1080 Ti GPU.

B.1 Numerical experiments for theories

Dataset We generated $n = 10,000$ samples following the model (3). We sampled $\tilde{\mathbf{D}} \in \mathbb{R}^{50 \times 100}$ from zero-mean Gaussian distribution, and then normalized the columns. The codes are 5-sparse with their support uniformly chosen at random and their amplitudes are sampled from Uniform(1, 2).

Training We let $T = 200$, and $\lambda = 0.2$ and $\alpha = 0.2$. The dictionary is initialized to $\tilde{\mathbf{D}} = \tilde{\mathbf{D}} + \tau_B \mathbf{B}$ with $\mathbf{B} \sim \mathcal{N}(\mathbf{0}, \frac{1}{m} \mathbf{I})$. For Figures 2, 3, 4a and 4b, we set $\tau_B \approx 0.55/\log m$. We picked this closeness to highlight the gradient directions in a closer neighbourhood of the dictionary. For Figures 4c and 4d, we chose much larger noise level, $\tau_B \approx 2.8/\log m$. The network is trained for 600 epochs with full-batch gradient descent using Adam optimizer [68] with learning rate of 10^{-3} and $\epsilon = 10^{-8}$. The learned dictionary is evaluated based on the error $\|\mathbf{D} - \tilde{\mathbf{D}}\|_2 / \|\tilde{\mathbf{D}}\|_2$. The results and conclusion were consistent across various realizations of the dataset and across various optimizers. Hence, in the main paper, the figures visualize results of one realization using Adam optimizer.

B.2 Dictionary learning

Dataset We generated $n = 50,000$ samples following the model (3). We let $m = 1000$ and $p = 1500$, and sample $\tilde{\mathbf{D}}$ from zero-mean Gaussian distribution, and then normalized the columns. The sparse codes \mathbf{z}^i are 10, 20, 40-sparse, where their supports are chosen uniformly at random and their amplitudes are sampled from Uniform(1, 2).

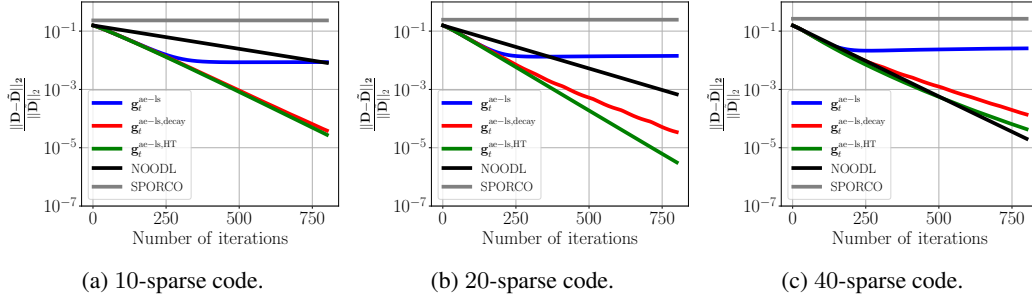


Figure 6: Dictionary learning convergence using g_t^{ae-ls} compared to NOODL [29] and SPORCO [65].

Training The dictionary is initialized to $\mathbf{D} = \tilde{\mathbf{D}} + \tau_B \mathbf{B}$ with $\mathbf{B} \sim \mathcal{N}(\mathbf{0}, \frac{1}{m} \mathbf{I})$ where $\tau_B \approx 1/\log m$. We let $\lambda = 0.2$, and $\alpha = 0.2$, and $T = 100$. The network is trained for 1,000 iterative updates with batch-size of 50 using Adam [68] with learning rate of 10^{-3} and $\epsilon = 10^{-3}$. For decay method, β is decreased in value by 0.005 every 100 update iterations. Each filter is normalized after every update. The learned dictionary is evaluated based on the relative error $\|\mathbf{D} - \tilde{\mathbf{D}}\|_2 / \|\tilde{\mathbf{D}}\|_2$.

B.3 Image denoising

Training We trained PUDLE where the dictionary is convolutional with 64 filters of size 9×9 and strides of 4. The encoder unfolds for $T = 15$, and the step size is set to $\alpha = 0.1$. Unlike the theoretical analysis where full-batch gradient descent is studied, the network is trained stochastically with Adam optimizer [68] with learning rate of 10^{-4} and $\epsilon = 10^{-3}$ for 250 epochs. At every training iteration, a random 129×129 patch is cropped and a zero-mean Gaussian noise with standard deviation of 25 is added. We report results in terms of the peak signal-to-noise-ratio (PSNR). The standard deviation of the test set PSNR across multiple noise realizations was lower than 0.02 dB for all the methods. Hence, we only reported the mean PSNR of the test set in the main paper.